molecules

MDPI

Article

An Unprecedented 4,8-Cycloeudesmane, Further New Sesquiterpenoids, a Triterpene, Steroids, and a Lignan from the Resin of *Commiphora myrrha* and Their Anti-Inflammatory Activity In Vitro

Anna Unterholzner [1], Katrin Kuck [1], Anna Weinzierl [1], Bartosz Lipowicz [2] and Jörg Heilmann [1,*]

[1] Institute of Pharmaceutical Biology, University of Regensburg, Universitätsstr. 31, D-93053 Regensburg, Germany; anna.unterholzner@chemie.uni-regensburg.de (A.U.)
[2] Repha GmbH Biologische Arzneimittel, Alt-Godshorn 87, D-30855 Langenhagen, Germany
* Correspondence: joerg.heilmann@chemie.uni-regensburg.de; Tel.: +49-941-9434761

Abstract: Myrrh has a long tradition in the treatment of inflammatory diseases. However, many of its (active) constituents are still unknown. In the present study, secondary metabolites were isolated from an ethanolic extract by various separation methods (liquid–liquid partition, silica and RP18 flash chromatography, CPC, and preparative HPLC), their structures were elucidated with NMR spectroscopy and mass spectrometry, and the selected compounds were tested for their effect on LPS-induced NO production by RAW 264.7 murine macrophages. Among the isolated substances are 17 sesquiterpenes (**1**–**17**) including the first 4,8-cycloeudesmane (**1**), a triterpene (**38**), two phytosterols (**39**, **40**) and one lignan (**43**), which were previously unknown as natural products. Numerous compounds are described for the first time for the genus *Commiphora*. Eight of the eleven compounds tested (**1**, **29**, **31**, **32**, **34**–**37**) showed a statistically significant, concentration-dependent weak to moderate anti-inflammatory effect on NO production in the LPS-stimulated RAW 264.7 macrophages in vitro. For the reference substance, furanoeudesma-1,3-diene, an IC_{50} of 46.0 µM was determined. These sesquiterpenes might therefore be part of the multi-target molecular principles behind the efficacy of myrrh in inflammatory diseases.

Keywords: *Commiphora myrrha*; Burseraceae; sesquiterpene lactone; cycloeudesmane; phytosterol; lignan; anti-inflammatory

Citation: Unterholzner, A.; Kuck, K.; Weinzierl, A.; Lipowicz, B.; Heilmann, J. An Unprecedented 4,8-Cycloeudesmane, Further New Sesquiterpenoids, a Triterpene, Steroids, and a Lignan from the Resin of *Commiphora myrrha* and Their Anti-Inflammatory Activity In Vitro. *Molecules* **2024**, *29*, 4315. https://doi.org/10.3390/molecules29184315

Academic Editor: Hinanit Koltai

Received: 9 August 2024
Revised: 27 August 2024
Accepted: 9 September 2024
Published: 11 September 2024

1. Introduction

The small trees or shrubs of the genus *Commiphora* (Burseraceae) grow in East Africa, the Arabian Peninsula, and India [1]. Their secreted oleo-gum resin, especially from *Commiphora myrrha* (Nees) Engl., is known as myrrh and consists of water-soluble gums, alcohol-soluble resin, and a volatile oil [2]. Numerous natural compounds from the resin have been described; sesquiterpenes and triterpenes were the predominant classes, each with multiple scaffolds [3]. Due to spectroscopic advances in the recent years, the identification of several dimeric sesquiterpenes has been described since 2018 [4–6]. Steroids are mainly found in *C. mukul* but have also been detected in *C. myrrha* [3,7]. The first lignans described for *C. myrrha* were of the bisepoxy or furofuran structural type [8].

Myrrh has been used since ancient times not only for cultural and religious purposes but also for the treatment of a variety of, often inflammatory, diseases [9]. Modern studies have demonstrated, in particular, the anti-inflammatory [10,11], anticancer [12], antibacterial [13,14] and analgesic [15,16] effect of the gum resin of *C. myrrha*. In addition, myrrh is established in the treatment of ulcerative colitis (UC) due to its positive effects in animal models [17] and in a clinical study in combination with coffee charcoal and chamomile flower extract [18]. Numerous studies have already shown that terpenoids

isolated from myrrh resin suppress inflammation in various experiments [11,19–21]. Despite the promising results and the indications that multiple sesquiterpenes are the main bioactive substances of myrrh [22], there are still unidentified active compounds and the molecular mechanisms of action are still insufficiently understood.

In the present study, an ethanolic extract of the drug was fractionated and several secondary metabolites were isolated. Furthermore, the anti-inflammatory effect of the selected substances in an in vitro model using RAW 264.7 macrophages is reported. Similar to human macrophages, this murine cell line produces nitric oxide (NO) as an immunomodulatory and toxic defence molecule during inflammation [23]. In an aqueous solution, NO autoxidizes to nitrite and can be quantified spectroscopically after staining with the Griess reagent. NO is one of the pathologically elevated factors in UC patients [24]. First, the evidence suggests that myrrh suppresses the inflammatory response in the in vitro model used by mediating haem oxygenase-1 expression [25]. In addition, myrrh suppressed the inflammation by influencing the MAPK signalling pathway in another cell model [11].

The aim of this work is therefore, on the one hand, to contribute to the phytochemical characterization of the secondary metabolites in myrrh, which is far from complete since it is a mixture of numerous minor components; and, on the other hand, to get a better understanding of its pharmacological principles of action.

2. Results

Myrrh resin was extracted with ethanol and the extract was split into two parts by a liquid–liquid partition between methanol and *n*-heptane. Both fractions were further separated using various chromatographic techniques such as flash chromatography, centrifugal partition chromatography (CPC), and preparative HPLC. The structures of the pure compounds were elucidated with NMR, mass spectrometry using liquid chromatography and high-resolution electrospray ionisation (HRESIMS), or gas chromatography combined with atmospheric pressure chemical ionisation (GC-APCI), and circular dichroism spectroscopy (CD). Thus, 37 sesquiterpenes, 1 triterpene, 4 phytosterols, and 1 lignan were identified, including 21 new natural products (**1**–**17**, **38**–**40**, and **43**) and 12 compounds that have not yet been described for the genus *Commiphora*. Known compounds that have not been described for *Commiphora* so far were elucidated by their NMR data to be serralactone A (**18**) [26], 1β,8β-dihydroxyeudesman-3,7(11)-dien-8α,12-olide (**19**) [27], neolitacumone B (**20**) [28], neolitacumone A (**21**) [27], 3-oxo-5α*H*,8β*H*-eudesma-1,4(15),7(11)-trien-8,12-olide (**22**) [29], (+)-eudebeiolide B (**23**) [30], linderolide I (**24**) [31], 1β,8β-dihydroxyeudesma-4,7(11)-dien-8α,12-olide (**25**) [32], istanbulin B and A (**26** and **27**) [33], chloraniolide A (**28**) [34], and 7-ketostigmasterol (**42**) [35]. For compounds **24** [31] and **28** [34], the additional literature data could be corrected. Stigmasta-5,22*E*-diene-3β,11α-diol (**41**) has been isolated from another species before, namely *C. mukul* [36].

In addition to compounds **1** and **21**, the following compounds known for *C. myrrha* were isolated and tested on their anti-inflammatory effects in the Griess assay: 2*S*-methoxy-4*S*-furanogermacra-1(10)*E*-en-6-one (**29**) [37,38], 2β-methoxyglechomanolide (**30**) [5], 8-*epi*-2β-methoxyglechomanolide (**31**) [5], isohydroxylindestrenolide (**32**) [39], hydroxylindestrenolide (**33**) [40], dehydrolindestrenolide (**34**) [41], 9-oxo-9,10-seco-isolindestrene (**35**) [5], alismol (**36**) [42], and commiterpene E (**37**) [5]. Furthermore, the known myrrh metabolites, 1(10)*E*,4*E*-furanodienone [43], 2-acetoxyfuranodiene [44], curzerenone [43], myrrhone [45] and 1*R*,2*R*-epoxy-4*S*-furanogermacr-10(14)-en-6-one [38,46] were isolated.

2.1. Sesquiterpenoids

The isolated sesquiterpenoids **1**–**37** are shown in Figure 1.

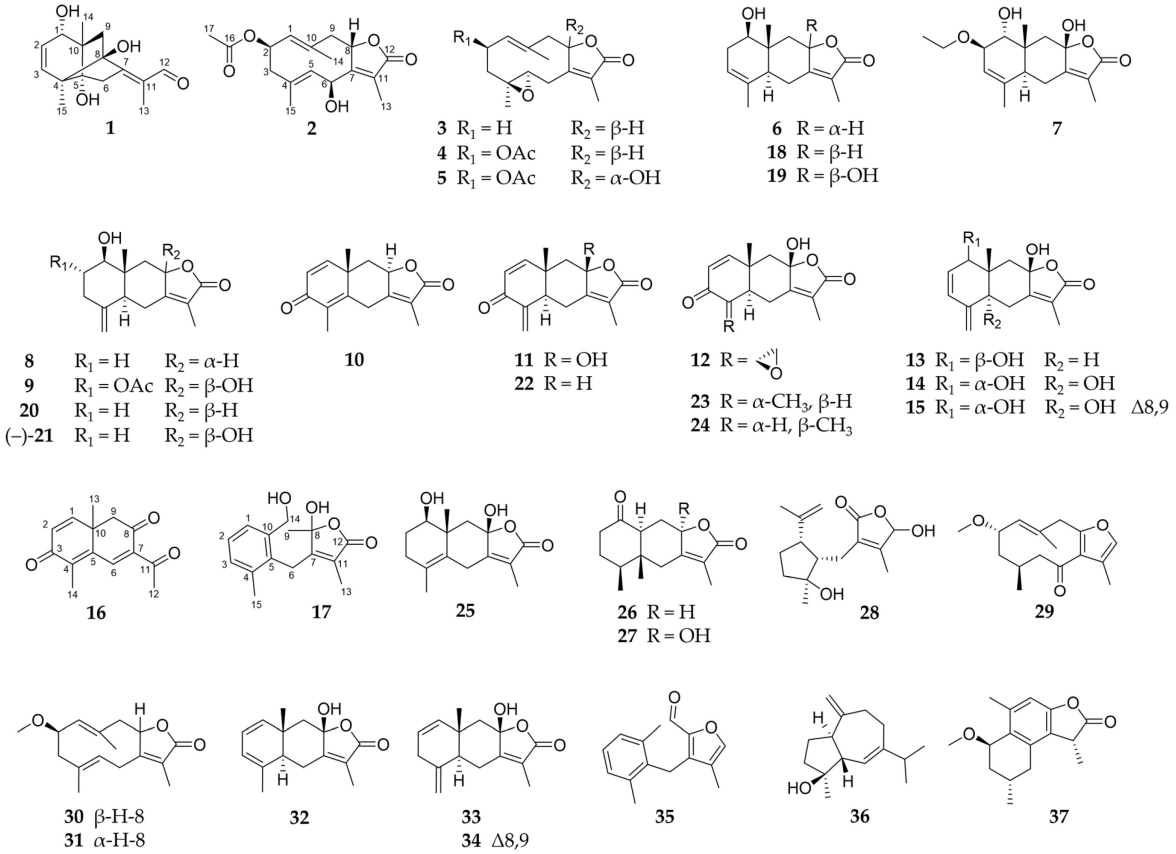

Figure 1. Chemical structures of the isolated sesquiterpenoids **1**–**37**.

Compound **1**, obtained as a colourless oil, showed a molecular formula of $C_{15}H_{20}O_4$, as determined by HRESIMS at *m*/*z* 265.1435 $[M+H]^+$ (calc. 265.1434). The NMR data of **1** (1D: Table 1, 2D: Figures 2 and 3, original spectra in Supplementary Materials Figures S1–S3) displayed 15 carbon resonances assignable to three methyls, two sp^3 methylenes, one oxygenated sp^3 methin, two sp^2 olefinic methins, an aldehyde moiety, and six quaternary carbons (two aliphatic, two hydroxylated, and two olefinic). There were six degrees of unsaturation evident in **1**, of which three were represented by one aldehyde group and two double bonds; therefore, the molecule is tricyclic. Since the COSY experiment only showed correlations between H-1/H-2 and H-2/H-3, the other hydrogenated carbons were neighboured by quaternary carbons, which was confirmed by the splitting pattern of their ^{1}H NMR signals. The HMBC correlations (Figure 2) of the exocyclic methyls H_3-14 and H_3-15 with the carbons adjacent to them via one and two bonds indicated the first cyclohexene ring. Further analysis of the 1D and 2D NMR data revealed an eudesmane-type skeleton with an additional bridging bond between C-4 and C-8 indicated by the HMBC signals between H_3-15/C-8 and H-9a/C-4. This structural type, which has not been described before, can be named as 4,8-cycloeudesmane. The HMBC cross-peaks also allowed for the assignment of an exocyclic 1-oxo-isopropyliden group at C-7. The relative stereochemistry of **1** was determined by its NOESY correlations (Figure 3). It was substantially conditioned by the bridged ring system, which was again confirmed by the correlations of H-9b with H-1 to H-3. The exocyclic double bond was *Z*-configured according to the signals between H_2-6/H_3-13, on the one hand, and H-9a/H-12, on the other hand. Consequently, the structure of 1β,5,8-trihydroxy-4α,8-cycloeudesma-2,7(11)*Z*-dien-12-al (**1**) was established, as shown in Figure 1.

Table 1. ^{1}H and ^{13}C NMR data of compounds **1**–**4** (**1**, **2**: 600 and 151 MHz; **3**, **4**: 400 and 101 MHz) in CD_3OD (δ in ppm, J in Hz, s: singlet, d: doublet, t: triplet, q: quartet, br: broad, and m: multiplet).

No.	1		2		3		4	
	δ_H	δ_C	δ_H	δ_C	δ_H	δ_C	δ_H	δ_C
1	3.61 (1H, d, 4.5)	76.6	5.00 (1H, d, 10.3)	132.2	4.87 (1H, brd, 11.6)	129.3	5.35 (1H, d, 10.4)	128.4
2	5.97 (1H, dd, 4.5, 9.8)	130.5	5.40 (1H, ddd, 5.0, 10.5, 10.5)	72.0	2.08 [a] (1H, m) 2.36 [a] (1H, m)	24.6	5.54 (1H, ddd, 5.0, 10.6, 11.2)	69.0
3	5.45 (1H, d, 9.7)	133.2	2.15 (1H, dd, 11.0, 11.0) 2.48 (1H, dd, 4.9, 11.3)	45.4	1.14 [a] (1H, m) 2.01 [a] (1H, m)	37.3	1.28 [a] (1H, m) 2.43 [a] (1H, m)	42.6
4		55.5		134.7		60.1		59.4
5		79.6	5.20 (1H, d, 7.3)	134.7	2.94 [a] (1H, m)	63.2	3.16 (1H, dd, 3.9, 8.4)	61.5
6	2.43 (1H, d, 18.7) 2.75 (1H, d, 18.7)	38.2	5.53 (1H, d, 7.3)	65.8	2.22 (1H, dd, 11.9, 14.9) 2.95 [a] (1H, m)	22.0	2.56 [a] (1H, m) 3.01 [a] (1H, m)	26.6
7		165.4		163.9		162.5		159.5
8		88.6	5.42 [a] (1H, m)	83.4	5.11 (1H, d, 6.0)	83.1	5.39 (1H, dd, 5.4, 6.2)	83.5
9	1.54 (1H, d, 12.5) 1.68 [a] (1H, d, 12.7)	47.8	2.79 (1H, dd, 6.1, 14.9) 2.91 (1H, dd, 2.3, 14.8)	42.7	2.54 [a] (1H, m) 2.64 [a] (1H, m)	38.6	2.40 [a] (1H, m) 3.00 [a] (1H, m)	40.5
10		43.2		137.1		127.4		133.5
11		131.3		127.5		124.4		126.5
12	10.68 (1H, s)	195.7		175.8		174.4		174.2
13	1.67 [a] (3H, s)	11.1	1.94 (3H, d, 1.7)	9.7	2.17 (3H, s)	12.4	1.80 (3H, brs)	8.0
14	1.20 (3H, s)	18.9	1.36 (3H, s)	17.1	1.67 (3H, brs)	18.6	1.69 (3H, brs)	17.9
15	1.02 (3H, s)	15.0	1.59 (3H, s)	18.7	1.16 (3H, s)	14.8	1.23 (3H, s)	16.8
16				172.4				170.6
17			2.01 (3H, s)	21.0			1.99 (3H, s)	19.5

[a] overlapped signal.

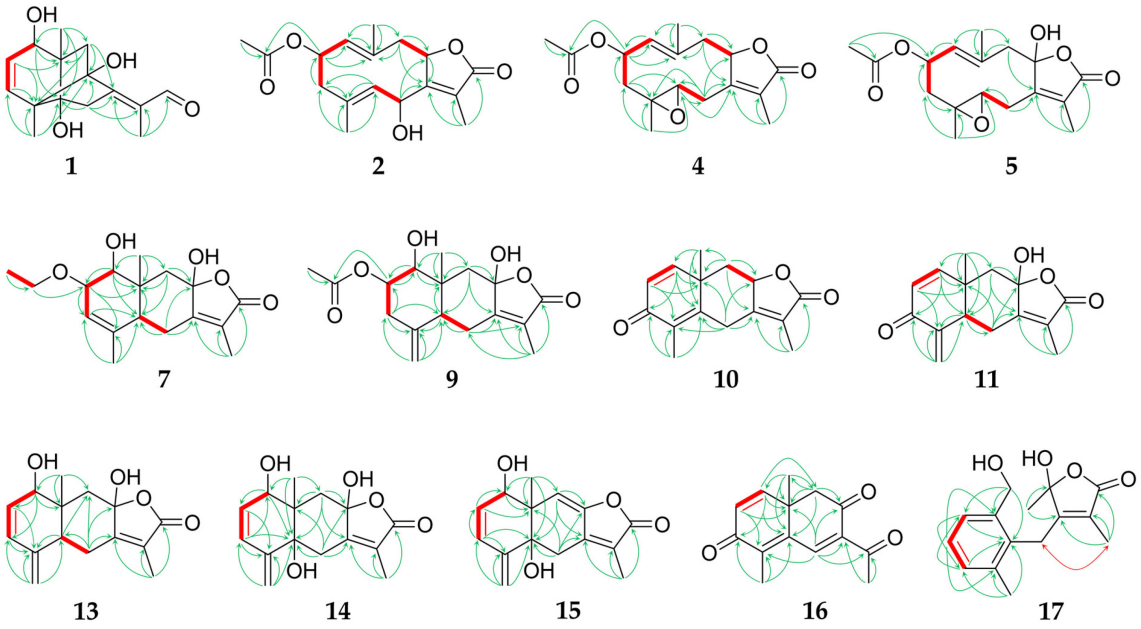

Figure 2. Key HMBC (green arrows) and COSY correlations (red, bold or red arrow) of sesquiterpenoid compounds with new constitution.

Compounds **2**–**5** can be summarized as the oxygenated derivatives of glechomanolide [47], with **2**, **4**, and **5** being derivatives of the known myrrh metabolite 2β-acetyloxyglechomanolide [39], and the molecular model calculated in the cited publication enabled the relative stereochemical characterization of the distant H-2 and H-8. According to the calculations and the observed signals of the substances, the characteristic NOESY correlations of 2β-acetyloxyglechomanolide derivatives were identified as follows: H_3-14 couples with H-2 and H-9α on the one side, and H-9β couples with H-1 and H-8 on the opposite side of the germacrene ring. In contrast, the C-8 epimeric compound as described by Greve et al. [39] showed cross-peaks between H_3-14 and not only H-2 but also, characteristically,

H-8. The replacement of the double bond at C-4 by an epoxidation in compounds **3**–**5** did not essentially change the conformation of the ten-membered germacrene ring, as observed in the corresponding NOESY data as well as described in the literature [48]. Compound **3** was lacking the 2-acetyloxy moiety, but its relative configuration could be established by comparing its NOESY signals with the otherwise identical compound **4**.

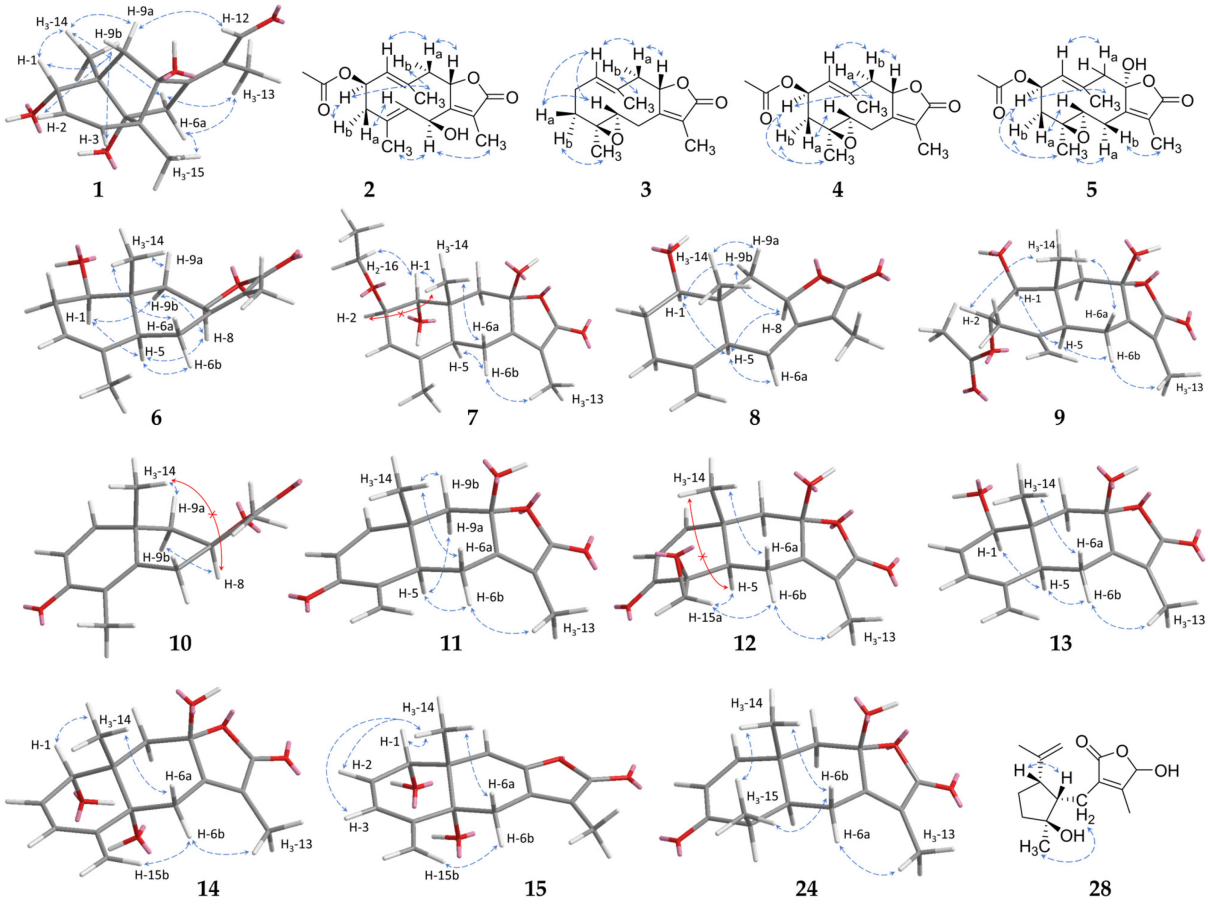

Figure 3. Key NOESY correlations (blue arrows, missing ones: red arrows) of chiral sesquiterpenoid compounds with new constitution or configuration. Three-dimensional structures were calculated using Chem3D where reasonable.

Compound **2** was obtained as a colourless oil and its molecular formula of $C_{17}H_{22}O_5$ was determined by HRESIMS at m/z 307.1545 $[M+H]^+$ (calc. 307.1540). Analysis of its 1D and 2D NMR spectra revealed that **2** is a C-6 hydroxylated derivative of 2β-acetyloxyglechomanolide [39] as shown by its chemical shifts (δ_H 5.53 (d, H-6); δ_C 65.8). In accordance with the calculated molecular models in the literature and the explanation above, the NOESY signals (Figure 3) indicated the relative stereochemical configurations at C-2 and C-8. They were furthermore confirmed by the CD spectrum of **2** with a prominent negative cotton effect at λ_{min} 214 nm ($\Delta\varepsilon$ –13.0; Figure S24) that was consistent with the spectra of 2β-acetyloxy- and 2β-methoxyglechomanolide in the literature [5]. The NOESY correlations of H-6 with H_3-13 but not H-8 confirmed the relative stereochemical configuration at C-6. Therefore, **2** was identified as 2β-acetyloxy-6β-hydroxyglechomanolide.

Compound **3** was isolated as a yellowish oil in mixture with compounds **4** and **22**, and its molecular formula of $C_{15}H_{20}O_3$ was determined by HRESIMS at m/z 249.1485 $[M+H]^+$ (calc. 249.1491). Investigation of its 1D and 2D NMR data revealed a diastereomeric derivate of 4α,5α-epoxy-1(10),7(11)-dienegermacr-8α,12-olide [49] with the opposite configuration at C-4 as the only difference. The associated *trans*-configuration of the epoxide in **3** was shown by NOESY correlations between H-3a/H-5, on the one hand, and H-3b/H_3-15,

on the other hand (Figure 3). The determination of the relative configuration at C-8 was enabled by the corresponding NOESY correlations to compound **4**, respectively, as generally described above and the cross-peaks of H-1 and H-5. In this way, **3** was elucidated as 4β,5α-epoxyglechomanolide.

Compound **4**, isolated as a yellowish oil in mixture with compounds **3** and **22**, showed a molecular formula of $C_{17}H_{22}O_5$ as determined by HRESIMS at *m*/*z* 307.1543 $[M+H]^+$ (calc. 307.1540). As indicated by its 1D and 2D NMR data, it represents the acetylated derivate of **3**, as well as the epoxidated derivative of 2β-acetyloxyglechomanolide [39]. NOESY signals as described above showed that **4** featured the same relative configuration at C-2 and C-8 (Figure 3). Furthermore, the correlations of H-3b with H-2 and H_3-15, on the one hand, and H-3a with H-5, on the other hand, helped to establish the *trans*-configuration of the epoxide. Consequently, the structure of **4** was elucidated as 2β-acetyloxy-4β,5α-epoxyglechomanolide.

Compound **5**, obtained as a white solid, had a molecular formula of $C_{17}H_{22}O_6$ as determined by HRESIMS at *m*/*z* 323.1492 $[M+H]^+$ (calc. 323.1489). Its 1D (Table 2) and 2D NMR spectra indicated a structure similar to **4** that was distinguished from it by an additional, α-oriented hydroxy group at C-8 (δ_C 106.0). Its relative configuration was determined based on the NOESY correlations between H-6b with H_3-13, on the one hand, and H-6a with H_3-15, on the other hand (Figure 3). The configuration corresponding to 8-*epi*-2β-methoxyglechomanolide and 8-*epi*-2β-acetyloxyglechomanolide [5] was confirmed by its similar CD spectrum showing a maximum at λ ($\Delta\varepsilon$) at 221 nm (+5.9) and a minimum at 245 nm (−5.0; Figure S24). The structure of **5** was thus identified as 2β-acetyloxy-4β,5α-epoxy-8-*epi*-hydroxyglechomanolide.

Table 2. ^{1}H and ^{13}C NMR data of compounds **5**–**7** (**5**, **6**: 400 and 101 MHz, **7**: 600 and 151 MHz) in CD_3OD (δ in ppm, *J* in Hz, s: singlet, d: doublet, t: triplet, q: quartet, br: broad, and m: multiplet).

No.	5		6		7	
	δ_H	δ_C	δ_H	δ_C	δ_H	δ_C
1	5.21 (1H, d, 9.7)	129.5	3.58 (1H, dd, 6.0, 10.4)	74.8	3.44 (1H, s)	74.9
2	5.64 (1H, m)	69.1	1.94–1.88 (1H, m) 2.20–2.12 (1H, m)	31.3	3.58 (1H, m)	80.6
3	1.27 (1H, dd, 10.7, 10.7) 2.46 (1H, dd, 5.2, 11.7)	41.7	5.36 (1H, dd, 1.0, 2.3)	120.5	5.50 (1H, m)	121.9
4		59.7		133.3		137.7
5	2.74 [a] (1H, m)	63.7	2.60 (1H, m)	40.8	2.26 [a] (1H, m)	42.9
6	2.35 (1H, dd, 8.8, 14.6) 2.74 [a] (1H, m)	22.8	2.49 (1H, dd, 12.9, 17.7) 2.86 (1H, ddq, 1.9, 3.7, 17.7)	25.0	2.31 (1H, dd, 12.5, 12.5) 2.96 (1H, dd, 2.8, 12.2)	24.6
7		159.0		164.4		162.9
8		106.0	5.20 (1H, ddq, 1.9, 8.0, 8.0)	78.3		106.3
9	2.40 (1H, d, 13.4) 2.97 (1H, d, 13.3)	50.4	1.40 (1H, dd, 6.6, 14.1) 2.43 (1H, dd, 10.9, 14.0)	40.5	1.96 (1H, d, 13.2) 2.01 (1H, d, 11.5)	46.3
10		133.8		38.0		38.5
11		129.5		120.2		122.8
12		171.5		176.0		174.5
13	1.89 (3H, s)	7.5	1.79 (3H, brs)	6.8	1.82 (3H, s)	8.0
14	1.99 (3H, s)	17.6	0.67 (3H, s)	12.8	1.11 (3H, s)	16.6
15	1.30 (3H, s)	16.9	1.70 (3H, s)	19.2	1.80 (3H, s)	21.4
16		170.6			3.55 (1H, dq, 7.1, 9.4) 3.65 (1H, dq, 7.1, 9.2)	65.8
17	1.99 (3H, s)	19.5			1.17 (3H, dd, 6.9, 6.9)	15.9

[a] overlapped signal.

Compound **6** was obtained as a colourless oil and its molecular formula of $C_{15}H_{20}O_3$ was determined by HRESIMS at *m*/*z* 249.1491 $[M+H]^+$ (calc. 249.1485). Evaluation of its 1D and 2D NMR data revealed the constitution of serralactone A [26] that was also isolated separately as compound **18**. However, the NOESY correlations (Figure 3) between H-5

and H-8 of **6** indicated the opposite configuration at C-8, such that **6** was determinable as 8-*epi*-serralacton A.

Compound **7**, isolated as colourless oil, had a molecular formula of $C_{17}H_{24}O_5$ as determined by HRESIMS at *m*/*z* 309.1698 $[M+H]^+$ (calc. 309.1697). Its NMR data showed signals for an ethyloxy substituent (δ_H 3.55/3.65 (dq/dq, H_2-16), 1.17 (dd, H_3-17); δ_C 65.8, 15.9, respectively) and the HMBC cross-peaks between H_2-16 and C-2 revealed its position (Figure 2). Apart from this moiety, the constitution as well as parts of the configuration of **7** were elucidated to be the same as for compound **19**, which is known as 1β,8β-dihydroxyeudesman-3,7(11)-dien-8α,12-olide [27]. The NOESY correlations of H-1 with H_3-14 and H_2-16 indicated the different relative configuration of **7** at C-1 (Figure 3). Notably, the ^{1}H NMR signal of H-1 appeared as a singlet despite its neighbouring hydrogen, which is explainable by their dihedral angle causing a coupling constant that is too small for resolution in the spectrum. Consequently, **7** can be named 1α,8β-dihydroxy-2β-ethyloxyeudesma-3,7(11)-dien-8α,12-olide.

Compound **8**, obtained as a yellowish oil, showed a molecular formula of $C_{15}H_{20}O_3$ as determined by HRESIMS at *m*/*z* 249.1490 $[M+H]^+$ (calc. 249.1491). The structure elucidated by its NMR spectra (Table 3) represents the H-8 epimer of neolitacumone B [28] that was also isolated as compound **20**. Based on the NOESY cross-peaks between H-5 and H-8 (Figure 3) that deviate from neolitacumone B, compound **8** was identified as 8-*epi*-neolitacumone B.

Table 3. ^{1}H and ^{13}C NMR data of compounds **8**–**11** (600 and 151 MHz, respectively) in CD_3OD (δ in ppm, *J* in Hz, s: singlet, d: doublet, t: triplet, q: quartet, br: broad, and m: multiplet).

No.	8		9		10		11	
	δ_H	δ_C	δ_H	δ_C	δ_H	δ_C	δ_H	δ_C
1	3.60 (1H, dd, 4.3, 11.6)	79.1	3.29 [a] (1H, m)	80.9	6.97 (1H, d, 9.9)	157.3	6.99 (1H, d, 10.0)	162.3
2	1.47 [a] (1H, m) 1.78 [a] (1H, m)	32.3	4.80 (1H, ddd, 6.0, 10.5, 11.9)	74.9	6.18 (1H, d, 9.9)	125.8	5.96 (1H, d, 9.9)	127.1
3	2.17 [a] (1H, m) 2.37 (1H, ddd, 2.4, 4.4, 13.7)	35.0	2.10 (1H, dd, 12.0, 12.0) 2.71 (1H, dd, 5.5, 12.8)	40.3		187.3		190.2
4		148.1		145.6		133.9		146.1
5	2.52 (1H, dd, 5.5, 12.7)	42.0	2.02 [a] (1H, m)	50.4		156.6	2.69 (1H, dddd, 2.4, 2.4, 2.4, 12.6)	50.7
6	2.69 (1H, ddq, 1.7, 5.1, 17.1) 2.81 (1H, dd, 12.7, 18.8)	25.5	2.48 (1H, dd, 12.5, 12.5) 2.73 (1H, dd, 4.2, 13.3)	24.7	3.79 (1H, s) 3.81 (1H, s)	29.1	2.56 (1H, dd, 13.5, 13.5) 2.96 (1H, dd, 2.9, 13.2)	24.6
7		165.0		162.2		162.2		160.6
8	5.19 (1H, ddq, 1.7, 9.3, 9.3)	79.6		105.4	4.93 (1H, m)	78.0		105.0
9	1.20 (1H, dd, 9.1, 13.9) 2.60 (1H, dd, 9.9, 13.9)	42.6	1.45 (1H, d, 13.7) 2.66 (1H, d, 13.6)	48.5	1.90 [a] (1H, m) 2.40 (1H, dd, 10.7, 14.0)	40.1	1.77 (1H, d, 13.3) 2.43 (1H, d, 13.4)	47.7
10		41.4		41.9		40.6		39.7
11		121.5		123.0		122.9		124.0
12		177.5		174.4		176.7		174.0
13	1.81 (3H, brs)	8.2	1.80 (3H, brs)	8.1	1.90 (3H, brs)	8.3	1.82 (3H, brs)	8.2
14	0.64 (3H, s)	15.2	1.03 (3H, s)	12.1	1.19 (3H, s)	27.9	1.24 (3H, s)	19.7
15	4.75 (1H, brs) 4.93 (1H, brs)	109.3	4.82 [a] (1H, s) 5.00 (1H, s)	110.7	1.94 (3H, s)	11.0	5.45 (1H, d, 2.1) 6.13 (1H, d, 1.7)	119.8
16				172.7				
17			2.04 (3H, s)	21.1				

[a] overlapped signal.

Compound **9** was obtained as a white solid and its molecular formula of $C_{17}H_{22}O_6$ was determined by HRESIMS at *m*/*z* 321.1344 $[M-H]^-$ (calc. 321.1344). Examination of its 1D and 2D NMR data revealed the C-2 acetylated derivative of neolitacumone A [27], which was also isolated as compound **21**. Therefore, the structure of 2α-acetyloxyneolitacumone A (**9**) was established as shown in Figure 1.

Compound **10**, obtained as yellowish oil, showed a molecular formula of $C_{15}H_{16}O_3$ as determined by HRESIMS at m/z 245.1174 $[M+H]^+$ (calc. 245.1172). The 1D and 2D NMR spectra revealed a so far unnamed and only synthetically obtained semichinoid eudesmanolide [50]. As only its ^{1}H NMR data have been published so far, the spectroscopic data of **10** were now completed during this study. Analogous to the known 3-oxo-5α*H*,8β*H*-eudesma-1,4(15),7(11)-trien-8,12-olide (**22**) [29], compound **10** was systematically named 3-oxo-8α*H*-eudesma-1,4,7(11)-trien-8,12-olide.

Compound **11** was obtained as a colourless oil and its molecular formula was determined to be $C_{15}H_{16}O_4$ by HRESIMS analysis at m/z 261.1126 $[M+H]^+$ (calc. 261.1121). Similar NMR data revealed an hydroxy-derivate of 3-oxo-5α*H*,8β*H*-eudesma-1,4(15),7(11)-trien-8,12-olide (**22**) [29], which was indicated by the downfield shifted signal of C-8 at δ_C 105.0. Compound **11**, which was consequently identified as 3-oxo-8β-hydroxy-5α*H*-eudesma-1,4(15),7(11)-trien-8,12-olide, could possibly represent a biosynthetic interstage between compounds **23** and **24** during the isomerization of the methyl C-15.

Compound **12**, obtained as yellowish oil, showed a molecular formula of $C_{15}H_{16}O_5$ as determined by HRESIMS at m/z 277.1067 $[M+H]^+$ (calc. 277.1071). Its constitution was determined by its 1D (Table 4) and 2D NMR data to be corresponding to linderolide J [31]. Notable was a deviation in the colour of the HSQC signals of the geminal H_2-15, both of which were blue. Examination of the NOESY correlations (Figure 3) of compound **12** revealed a diastereomer with an opposite configuration at the spiro carbon C-4, which was indicated by the signals between H-5 and H-15a in the exocyclic oxirane ring. Thus, **12** was elucidated to be 4-*epi*-linderolide J.

Table 4. ^{1}H and ^{13}C NMR data of compounds **12**–**14** (600 and 151 MHz, respectively) in CD_3OD (δ in ppm, J in Hz, s: singlet, d: doublet, t: triplet, q: quartet, br: broad, and m: multiplet).

No.	12		13		14	
	δ_H	δ_C	δ_H	δ_C	δ_H	δ_C
1	7.14 (1H, d, 10.1)	163.2	4.00 (1H, s)	78.8	3.58 (1H, d, 5.3)	74.5
2	6.03 (1H, d, 10.0)	127.1	5.53 (1H, d, 9.9)	132.8	5.88 (1H, dd, 5.2, 10.1)	128.9
3		195.3	6.17 (1H, dd, 9.9, 2.8)	131.3	6.19 (1H, d, 9.8)	129.6
4		58.3		145.7		147.8
5	2.57 (1H, dd, 3.5, 13.8)	46.4	2.17 [a] (1H, m)	47.3		78.2
6	2.37 (1H, dd, 13.0, 13.0) 2.57 (1H, dd, 3.5, 13.8)	21.6	2.41 (1H, dd, 13.8, 13.8) 2.92 (1H, dd, 3.8, 13.2)	24.8	2.68 (1H, brd, 13.8) 3.06 (1H, d, 13.6)	32.1
7		160.6		162.0		160.2
8		104.8		105.4		106.2
9	1.77 (1H, d, 13.3) 2.41 (1H, d, 13.9)	48.0	1.48 (1H, d, 13.7) 2.66 (1H, d, 13.6)	49.0	1.93 (1H, d, 13.7) 2.57 (1H, d, 13.7)	41.5
10		38.8		41.6		41.8
11		124.1		122.9		125.8
12		173.9		174.4		174.6
13	1.81 (3H, brs)	8.1	1.81 (3H, brs)	8.1	1.81 (3H, brs)	8.2
14	1.45 (3H, s)	22.7	0.95 (3H, s)	11.9	1.07 (3H, s)	22.0
15	3.09 (1H, d, 5.5) 3.28 (1H, d, 5.6)	46.9	4.99 (1H, s) 5.03 (1H, s)	112.1	5.16 (1H, s) 5.33 (1H, s)	114.3

[a] overlapped signal.

Compound **13**, obtained as a white solid, showed a molecular formula of $C_{15}H_{18}O_4$ as determined by HRESIMS at m/z 263.1277 $[M+H]^+$ (calc. 263.1278). By its 1D and 2D NMR spectra, a derivative of neolitacumone A (**21**) was elucidated with an additional double bond in the position C-2 as indicated by the chemical shifts. Similar to **7**, the following deviations from the usual ^{1}H NMR signal multiplicities were observed: H-1 and H-2 showed reductions to a singlet and a doublet, respectively, due to a very small coupling constant. In contrast, H-3 appeared as doublet of doublet with H-1 via the double bond, as established by an intense COSY cross-peak; however, this coupling again did not show

up in the H-1 multiplicity. The positions of the carbons in this order were established by the HMBC signal of H_2-15 with C-3 (Figure 2), as well as by the NOESY signals between H-1/H-2 and H-3/H-15b (Figure 3). For compound **13**, the name 1β,8β-dihydroxy-5α*H*-eudesma-2,4(15),7(11)-trien-8,12-olide is proposed.

Compound **14**, obtained as a white solid, showed a molecular formula of $C_{15}H_{18}O_5$ as determined by HRESIMS at *m*/*z* 279.1226 $[M+H]^+$ (calc. 279.1227). Investigation of its 1D and 2D NMR data revealed a trihydroxylated eudesmanolide differing from **13** by an additional hydroxy group at C-5 (δ_C 78.2), as well as the relative stereochemical configuration at C-1, according to the NOESY correlation of H-1 with H_3-14 (Figure 3). The remaining stereo centres were also determined by the NOESY cross-peaks in combination with molecular models obtained with Chem3D; for the opposite configuration at C-5, the calculated distance of 4,9 Å between H_3-14 and H-6a would prohibit the intense NOESY signal that was observed. Consequently, compound **14** was identified as 1α,5α,8β-trihydroxyeudesma-2,4(15),7(11)-trien-8,12-olide.

Compound **15**, obtained as a yellowish oil, showed a molecular formula of $C_{15}H_{16}O_4$ as determined by HRESIMS at *m*/*z* 261.1125 $[M+H]^+$ (calc. 261.1121). The 1D (Table 5) and 2D NMR data suggested a molecule related to **14**, which differs from it by the elimination of a water molecule, resulting in a double bond between C-8 (δ_C 147.9) and C-9 (δ_C 112.1). The relative stereochemical configuration at C-5, respectively, the *trans* configuration of the annulated cyclohexenes, could be determined by the NOESY signals of H_3-14 with H-1 and H-2, in accordance with their distance being less than 4 Å only in this configuration according to the Chem3D calculations (Figure 3). Therefore, the structure of 1α,5α-dihydroxyeudesma-2,4(15),7(11),8-tetraen-8,12-olide (**15**) was established as shown in Figure 1.

Table 5. ^{1}H and ^{13}C NMR data of compounds **15**–**17** and **24** (**17**: 600 and 151 MHz; **15**, **16** and **24**: 400 and 101 MHz) in CD_3OD (**15**–**17**) or $CDCl_3$ (**24**) (δ in ppm, *J* in Hz, s: singlet, d: doublet, t: triplet, q: quartet, br: broad, and m: multiplet).

No.	15		16		17		24	
	δ_H	δ_C	δ_H	δ_C	δ_H	δ_C	δ_H	δ_C
1	3.93 (1H, d, 5.3)	72.5	7.08 (1H, d, 9.9)	155.6	7.26 (1H, d, 7.7)	127.5	6.81 (1H, d, 9.9)	158.6
2	5.91 (1H, dd, 5.3, 9.9)	126.9	6.34 (1H, d, 9.9)	126.4	7.19 (1H, dd, 7.4, 7.4)	128.3	5.91 (1H, d, 10.1)	126.0
3	6.25 (1H, d, 9.9)	128.7		185.6	7.15 (1H, d, 7.1)	130.8		201.6
4		145.6		139.6		139.1	2.62 [a] (1H, m)	44.2
5		75.2		149.0		134.1	2.11 (1H, dd, 3.0, 6.0, 13.3)	46.4
6	2.93 (1H, dq, 1.8, 17.3) 3.16 (1H, d, 17.2)	29.3	8.24 (1H, s)	143.5	3.87 (2H, brs)	27.6	2.50 (1H, dd, 3.0, 13.5) 2.68 [a] (1H, m)	25.5
7		146.6		137.1		161.0		159.3
8		147.9		194.8		107.6		103.0
9	5.76 (1H, s)	112.1	2.68 (2H, d, 5.7)	48.5	1.48 (3H, s)	24.3	1.70 (1H, d, 13.6) 2.34 (1H, d, 13.4)	49.6
10		43.5		41.2		141.3		36.9
11		121.8		197.7		124.8		122.7
12		171.8	2.49 (3H, s)	29.3		174.3		171.1
13	1.91 (3H, brs)	6.9	1.32 (3H, s)	25.9	1.21 (3H, s)	7.7	1.84 (3H, brs)	8.4
14	0.99 (3H, s)	22.2	2.15 (3H, s)	10.0	4.63 (2H, s)	63.7	1.46 (3H, s)	22.5
15	5.22 (1H, s) 5.39 (1H, brs)	113.6			2.29 (3H, s)	20.0	1.27 (3H, d, 8.2)	13.4

[a] overlapped signal.

Compound **16** was obtained as a yellowish oil and showed a molecular formula of $C_{14}H_{14}O_3$ as determined by HRESIMS at *m*/*z* 231.1017 $[M+H]^+$ (calc. 231.1016). Its 1D and 2D NMR data indicated a norsesquiterpenoid structure similar to tussfarfarin A [51] with a

missing C-13. The measured NMR spectra showed an additional double bond between C-1 and C-2 (δ_H 7.08 (d, H-1), 6.34 (d, H-2); δ_C 155.6, 126.4, respectively) as well as a keto group at C-8 (δ_C 194.8) as structural differences to tussfarfarin A. Consequently, the molecule was identified as 1,2-anhydro-8-oxo-tussfarfarin A (**16**).

Compound **17** was isolated as a white solid and had a molecular formula of $C_{15}H_{18}O_4$ as determined by HRESIMS at m/z 263.1274 $[M+H]^+$ (calc. 263.1278). As indicated by its NMR data, it was a secoeudesmanolide similar to the previously described 9,10-seco-isolindestrenolide [5], differing in two additional hydroxylations at C-8 and C-14. Therefore, the name 8,14-dihydroxy-9,10-seco-isolindestrenolide is suggested.

Identical NMR data revealed **21** to be neolitacumone A, which showed a positive rotation when isolated from *Neolitsea acuminatissima* [27]. The measured optical rotation has an opposite sign (−7.3, in MeOH). Therefore, the isolation of (–)-neolitacumone A is postulated.

Compound **24**, obtained as yellowish oil, showed a molecular formula of $C_{15}H_{18}O_4$ as determined by HRESIMS at m/z 263.1281 $[M+H]^+$ (calc. 263.1278). It was established by its 1D and 2D NMR signals to have the chemical structure and relative configuration of linderolide I [31]. As key NOESY signals for the relative stereochemical characterisation, correlations between H_3-14 and H_3-15 with H-6b, on the one hand, and H-6a and H_3-13, on the other hand, were used to determine C-8 (Figure 3). However, the ^1H and ^{13}C NMR signals (both in $CDCl_3$) as well as the CD spectrum (Figure S25) are deviant from the literature data. Therefore, the determination of the configuration at C-8 performed by Liu et al. [31] by the interpretation of the CD spectrum has to be doubted.

For compound **28**, obtained as a yellowish oil, a molecular formula of $C_{15}H_{22}O_4$ was determined by HRESIMS at m/z 267.1595 $[M+H]^+$ (calc. 267.1591). Its NMR data were identical to those of chloraniolide A [34], and the elucidation revealed a secoguaianolide with the same constitution. Thereby, the missing HSQC signal between C-12 and H-12 stood out; however, H-12 showed COSY and NOESY correlations with H_3-13 (Figure 3). Regarding the relative stereochemical configuration, the NOESY correlations of H_3-15 were more intense with H_2-6 than with H-5. Therefore, the at C-4 epimeric structure of chloraniolide A published by Xu et al. [34] was determined to be its true configuration, so that its structure can be corrected. The stereo centre at C-12 cannot be determined based on the NOESY data due to its distance, as in the cited publication.

2.2. Further Structural Types

The structures of the isolated triterpene (**38**), the phytosterols (**39**–**42**) characterized by an extended side chain, and the lignan (**43**) are presented in Figure 4.

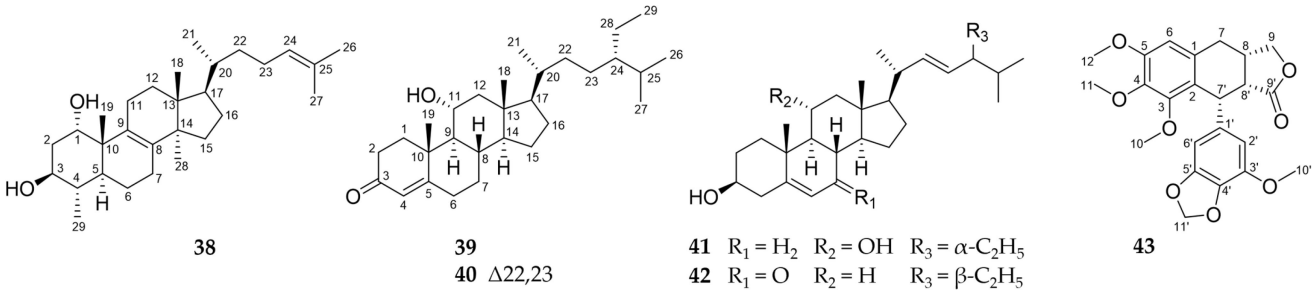

Figure 4. Chemical structures of the isolated triterpene (**38**), the phytosterols (**39**–**42**), and the lignan (**43**).

Compound **38** was obtained as a white solid. Its molecular formula of $C_{29}H_{48}O_2$ was determined by GC-APCI at m/z 429.3727 $[M+H]^+$ (calc. 429.3727). The NMR data (1D: Table 6) of the isolated compound showed a lot of similarities to the already known 29-norlanost-8,24-dien-1α,2α,3β-triol [52]. In contrast to this substance, **38** showed no hydroxylation at C-2 (δ_H 1.67/2.08 (ddd/m, H_2-2); δ_C 36.3). Thus, the substitution pattern

in the A ring matches the other triterpenes isolated from *C. myrrha* like cycloartan-24-ene-1α,3β-diol [53]. Due to strong NOESY signals below the ring level between H-3, H-2b, and H-29 as well as above the ring level between H-1, H-2a and H-19 (Figure 5), a relative 1α,3β-configuration could be assigned to the substance in accordance with the similar molecules mentioned above. To the best of our knowledge, this is the first description of this triterpene and, in accordance with trivial nomenclature, the name 29-norlanost-8,24-dien-1α,3β-diol is suggested.

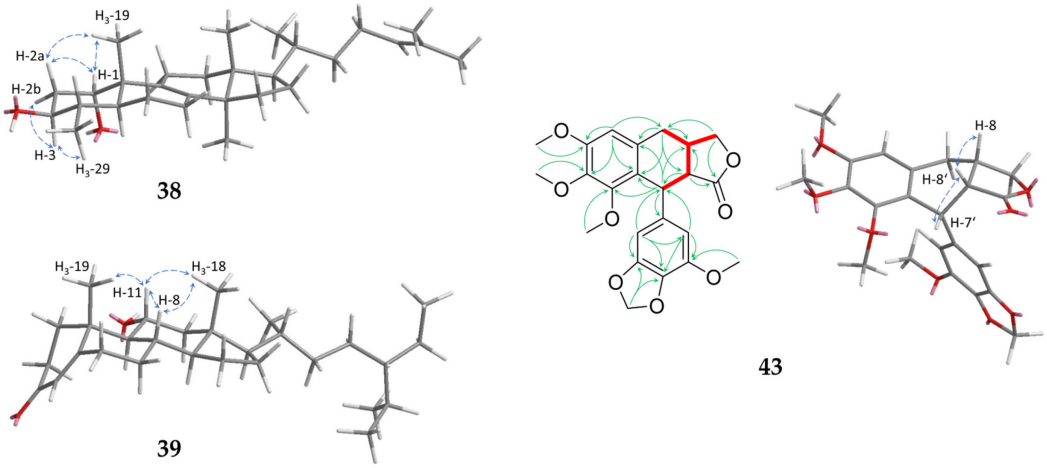

Figure 5. Key NOESY (blue arrows) correlations of compounds **38**, **39**, and **43** as well as HMBC (green arrows) and COSY correlations (red, bold) of **43**.

Compound **39**, obtained as a colourless oil, showed a molecular formula of $C_{29}H_{48}O_2$ as determined by GC-APCI at m/z 429.3728 $[M+H]^+$ (calc. 429.3727). The NMR data of **39** showed great similarities to previously isolated phytosterols [54] but also differences in the hydroxylation pattern. Whereas the substances described in the literature have a hydroxy group in 12β-position, this moiety is shifted to C-11 in **39**. This is indicated by COSY correlations between H-11 and H-9, while the signals between H_2-12 and H-9 are missing. The HMBC data display a similar pattern with strong correlations of H-12a (δ_H 1.24) to C-18 and H-12b (δ_H 2.30) to C-14. Thus, the hydroxy group can be unambiguously located at C-11. Based on strong NOESY correlations above the ring level between H-11 and the protons H-8, H_3-18, and H-19, an α-configuration at position 11 could be established (Figure 5). Thus, **39** was elucidated to be 11α-hydroxysitost-4-en-3-one.

Compound **40** was obtained as a white solid and its molecular formula of $C_{29}H_{46}O_2$ determined by GC-APCI at m/z 427.3570 $[M+H]^+$ (calc. 427.3571). Its NMR data show many similarities to **39** indicating the same substitution pattern in the steroidal annulated ring system. In contrast, the signals of the side chain included typical chemical shifts in the lower field, indicating the presence of another double bond between C-22 and C-23 as also present in **41** and **42**. Therefore, the structure of 11α-hydroxystigmast-4-en-3-one was established as shown in Figure 4.

Compound **43** was obtained as a yellowish solid and showed a molecular formula of $C_{23}H_{24}O_8$ as determined by HRESIMS at m/z 429.1547 $[M+H]^+$ (calc. 429.1544). On the basis of its NMR spectra (Table 7), it was elucidated as a stereoisomer of a previously synthetically obtained multiple methoxylated aryltetralin lignanolide [55]. Intense NOESY correlations between H-8′ and H-8 as well as H-7′ indicated their positions on the same side of the ring (Figure 5). Taking into account the biosynthetic origin as dimeric phenylpropanoid, we suggest the name *rel*-7′-(3′-methoxy-4′,5′-methylendioxyphenyl)-3,4,5-trimethoxy-7,8*S*,7′*R*,8′*R*-tetrahydronaphtho[2,3-c]furan-9′(3*H*)-one for **43**.

Table 6. ^{1}H and ^{13}C NMR data of compounds **38**–**40** (600 and 151 MHz, respectively) in $CDCl_3$ (δ in ppm, *J* in Hz, s: singlet, d: doublet, t: triplet, q: quartet, br: broad, and m: multiplet).

No.	38		39		40	
	δ_H	δ_C	δ_H	δ_C	δ_H	δ_C
1	3.97 (1H, dd, 3.0, 3.0)	72.7	1.98 [a] (1H, m) 2.67 (1H, ddd, 4.5, 4.5, 14.2)	37.6	2.00 (1H, ddd, 4.4, 13.8, 13.8) 2.67 (1H, ddd, 4.5, 4.5, 14.2)	37.6
2	1.67 (1H, ddd, 2.6, 11.1, 13.6) 2.08 [a] (1H, m)	36.3	2.32 (1H, ddd, 4.5, 4.5, 17.2) 2.44 (1H, ddd, 4.8, 14.2, 17.2)	34.2	2.33 (1H, ddd, 4.3, 4.3, 17.2) 2.45 (1H, ddd, 4.7, 13.5, 17.3)	34.2
3	3.55 (1H, ddd, 5.1, 9.5, 11.4)	72.3		200.2		200.2
4	1.44 [a] (1H, m)	38.6	5.73 (1H, s)	124.5	5.73 (1H, s)	124.5
5	1.45 [a] (1H, m)	40.1		171.3		171.2
6	1.32 [a] (1H, m) 1.80 [a] (1H, m)	19.9	2.27 [a] (1H, m) 2.36 (1H, ddd, 5.1, 14.2, 14.2)	33.7	2.27 [a] (1H, m) 2.37 (1H, ddd, 5.0, 14.3, 14.3)	33.7
7	2.15 (2H, m)	21.4	1.06 [a] (1H, m) 1.83 (1H, m)	31.6	1.05 [a] (1H, m) 1.83 (1H, dddd, 2.8, 2.8, 5.2, 12.9)	31.6
8		141.3	1.51 [a] (1H, dd, 12.9, 12.9)	34.9	1.52 [a] (1H, m)	35.0
9		129.2	1.08 (1H, dd, 10.8, 10.8)	59.3	1.08 [a] (1H, m)	59.3
10		42.2		39.9		39.9
11	2.06 (2H, m)	26.2	4.01 (1H, m)	69.3	4.02 (1H, ddd, 5.2, 10.7, 15.7)	39.2
12	1.79 [a] (2H, m)	30.9	1.24 [a] (1H, m) 2.30 [a] (1H, m)	51.9	1.26 [a] (1H, m) 2.28 [a] (1H, m)	51.8
13		44.5		43.1		43.0
14		50.3	1.13 [a] (1H, m)	55.3	1.21 [a] (1H, m)	55.8
15	1.21 (1H, ddd, 1.9, 9.6, 11.8) 1.61 [a] (1H, m)	30.8	1.10 [a] (1H, m) 1.61 [a] (1H, m)	24.1	1.09 [a] (1H, m) 1.58 [a] (1H, m)	24.1
16	1.33 [a] (1H, m) 1.93 [a] (1H, m)	28.0	1.26 [a] (2H, m)	29.7	1.30 [a] (1H, m) 1.76 (1H, dddd, 5.4, 9.0, 9.0, 14.0)	28.9
17	1.51 [a] (1H, m)	50.3	1.17 [a] (1H, m)	55.9	1.15 [a] (1H, m)	55.4
18	0.72 (3H, s)	15.7	0.75 (3H, s)	13.2	0.77 (3H, s)	13.3
19	1.01 (3H, s)	19.0	1.32 (3H, s)	18.3	1.32 (3H, s)	18.3
20	1.40 [a] (1H, m)	36.2	1.37 [a] (1H, m)	36.1	2.04 [a] (1H, m)	40.4
21	0.93 (3H, d, 6.6)	18.7	0.94 (3H, d, 6.1)	18.6	1.04 (3H, d, 6.6)	21.1
22	1.05 [a] (1H, m) 1.42 [a] (1H, m)	36.4	1.02 [a] (1H, m) 1.32 [a] (1H, m)	33.7	5.13 (1H, dd, 8.5, 15.1)	137.7
23	1.86 [a] (1H, m) 2.04 [a] (1H, m)	24.9	1.16 [a] (2H, m)	26.0	5.04 (1H, dd, 8.8, 14.9)	129.5
24	5.10 [a] (1H, dd, 7.2, 7.2)	125.2	0.93 [a] (1H, m)	45.7	1.54 [a] (1H, m)	51.2
25		131.2	1.66 [a] (1H, m)	29.1	1.54 [a] (1H, m)	31.0
26	1.60 (3H, s)	17.6	0.81 (3H, d, 6.6)	19.0	0.80 [a] (3H, m)	19.0
27	1.68 (3H, s)	25.7	0.84 [a] (3H, m)	19.8	0.85 (3H, d, 6.6)	21.1
28	0.92 [a] (3H, s)	25.1	1.23 [a] (1H, m) 1.27 [a] (1H, m)	23.0	1.17 [a] (1H, m) 1.43 [a] (1H, m)	25.4
29	1.02 [a] (3H, d, 5.5)	115.0	0.84 [a] (3H, m)	12.0	0.80 [a] (3H, m)	12.2

[a] overlapped signal.

Table 7. ^{1}H and ^{13}C NMR data of compound **43** (600 and 151 MHz, respectively) in CD_3OD (δ in ppm, *J* in Hz, s: singlet, d: doublet, t: triplet, q: quartet, br: broad, and m: multiplet).

No.	43	
	δ_H	δ_C
1		132.5
2		124.9
3		152.6
4		142.3
5		154.2
6	6.67 (1H, s)	109.7
7	2.51 (1H, dd, 1.9, 15.7) 2.75 (1H, dd, 7.7, 15.4)	32.9
8	3.18 (1H, m)	33.4
9	3.92 (1H, dd, 3.3, 9.4) 4.49 (1H, dd, 7.8, 9.1)	75.1
10	3.76 (3H, s)	61.6
11	3.82 (3H, s)	61.3
12	3.85 (3H, s)	56.5
1′		137.8
2′	6.35 (1H, brs)	108.7
3′		144.9
4′		135.1
5′		150.6
6′	6.29 (1H, brs)	102.4
7′	4.83 [a] (1H, m)	39.7
8′	3.62 (1H, dd, 2.2, 9.9)	46.3
9′		181.3
10′	3.79 (3H, s)	57.4
11′	5.86 (1H, s) 5.92 (1H, s)	102.5

[a] overlapped signal.

2.3. Activity against NO Production

For the investigation of the anti-inflammatory principle of myrrh, sesquiterpenes obtained in a sufficient HPLC-DAD purity (>90%) (**1**, **21**, **29**–**37**; ^{1}H and ^{13}C NMR spectra in Supplementary Materials Figures S1 and S28–S37) as well as the reference substance, furanoeudesma-1,3-diene (FUR), were selected. They were evaluated for their activity against NO production in LPS-stimulated RAW 264.7 murine macrophages in vitro using the Griess reagent (Figure 6). Non-toxic concentrations that affect cell viability by less than 10% were previously determined by MTT assays (Figure S27).

Eight of the eleven tested compounds (**1**, **29**, **31**, **32**, **34**–**37**) as well as FUR showed concentration-dependent slight but significant reductions in NO release by up to 40% (**37**; Figure 6). The strongest activity was shown by compound **34** with a reduction in NO synthesis to 63% at a concentration of 10 µM. Interestingly, FUR was the fourth most active compound when comparing the results at a concentration of 25 µM but was the only one showing a reduction by more than 50% percent in a non-toxic concentration range. Therefore, its IC_{50} value could be calculated by nonlinear regression analysis to be 46.0 µM, which can be classified as moderate activity (Figure 7).

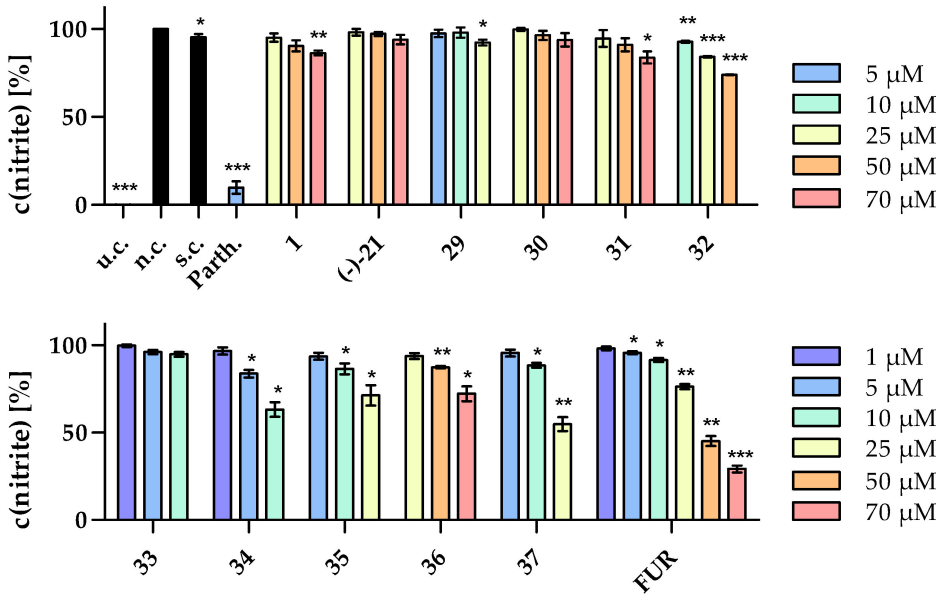

Figure 6. Influence of compounds **1**, (−)-**21**, **29**–**37**, and furanoeudesma-1,3-diene (FUR) on LPS-induced (1 µg/mL) NO production by RAW 264.7 macrophages in the Griess assay. The tests were performed in hexaplicates including an untreated control (u.c., medium without LPS), a negative control (n.c.), a solvent control (s.c., 0.1% DMSO, *v*/*v*), and a positive control (parthenolide, 5 µM). Data are presented as mean ± SEM, * $p < 0.05$, ** $p < 0.01$, *** $p < 0.001$ vs. n.c. (student's *t*-test, $n = 3$).

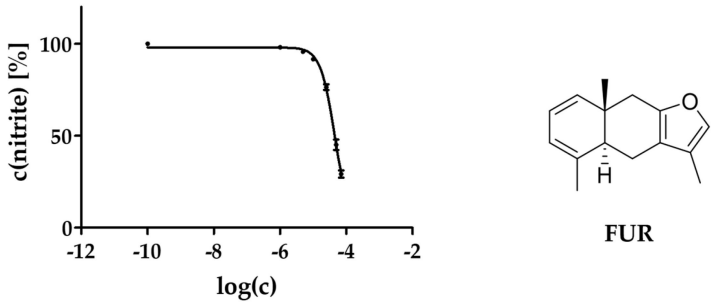

Figure 7. Influence of different concentrations of FUR on LPS-induced NO production by RAW 264.7 macrophages (IC_{50} = 46.0 µM). The tests were performed in hexaplicates ($n = 3$) and the data are presented as mean ± SEM including nonlinear regression curve. c in mol/L.

3. Discussion and Conclusions

3.1. Structural Diversity

The terpenoids, phytosterols, and the lignan presented here contribute to the still far from complete phytochemical characterization of myrrh and illustrate the heterogeneity of the resin. Most of the compounds isolated from *C. myrrha* in the present work were eudesmanolides, but germacranes, a noreudesmane, a secoeudesmane, two eremophilanes, a secoguaiane, a triterpene, phytosterols and a lignan were also found. In addition, the structures varied in multiple functionalities including a rare ethyloxy substitution (**7**). With compound **1**, the first 4,8-cycloeudesmane type sesquiterpene was elucidated. Compound **16** represents the first norsesquiterpenoid, and compounds **26** and **27** were the first eremophilanes described for *Commiphora* sp. With **43**, the first aryltetralin lignan was found for *C. myrrha*. The analysis of the rich secondary metabolite spectrum is not only crucial for the quality analytics of the drug but also the basis for identifying the molecular principle of action, and it may even be useful for general drug discovery.

Overbridged ring systems as present in the new 4,8-cycloeudesmane structural type in compound **1** have been described for *C. myrrha*. With α-copaene und β-ylangene, two 5,10-cyclocadinanes are known constituents of its essential oil [56]. In other plants,

cycloeudesmanes with additional covalent bonds between C-1 and C-3, C-2 and C-4, C-5 and C-7, as well as between C-6 and C-8 have been found [57,58].

The structural class of secoeudesmanes was recently discovered through our work on *C. myrrha* [21]. The introduced compound **17** is another representative of this class. Compound **28** is also formed by a cleavage step in the biosynthesis resulting in a rare secoguaiane scaffold. In addition, 7,8-secocadinanes are also known for *C. myrrha* [59].

Within the species *Commiphora*, steroids are dominating in *C. mukul* [3]. With β-sitostenone and β-sitosterol, two phytosterols were described for *C. myrrha* [7]. The four phytosterols **39**–**42** found in the present study extend the known spectrum and thus provide evidence for their possible contribution to bioactivity as a generally active structural class [60].

Further lignans of the aryltetralin type, as present in **43**, have been described for *C. incisa* [61] and *C. erlangeriana* [62]. Two of them, the erlangerins C and D, are known to be toxic and show the same substitution pattern of the aromatic rings as present in podophyllotoxin [63]. For *C. myrrha*, only lignans of the bisepoxy (or furofuran) structural type have been described so far [8].

3.2. Anti-Inflammatory Activity

The weakly to moderately active compounds presented might be part of the multi-target molecular principles behind myrrh's efficacy in inflammatory diseases in general, as well as, in particular, in UC patients with increased NO levels. The results therefore support the evidence that multiple sesquiterpenes are the bioactive principles of myrrh [22]. Further investigations are necessary, however, to clarify their structure–activity relationship(s) as well as their target(s) and the principles of the effectiveness of myrrh in humans. Synergistic effects between the compounds may also be involved, as they have been described for the combination of myrrh with frankincense [22] or with chamomile flower extract and coffee charcoal [64].

Apart from our results, the known compounds **19**, **21**, **25** [32], **23** [65] and **36** [66] were described in the literature as active NO inhibitors in the Griess assay. The published data were reproduced in parts for **36**, as a significant reduction was measured; the ineffectiveness of **21** could maybe attributed to its stereochemistry as possibly the (+)-enantiomer was tested to be active by Liu et al. [32].

The active reference substance FUR represents one of the main components of *C. myrrha*'s volatile oil with a proportion of up to 30% [67,68]. Its moderate inhibitory activity on the expression of the intercellular adhesion molecule 1 (ICAM-1) in vitro has been shown [21], as well as the analgesic effects via the opioid receptors in mice [69].

The observed anti-inflammatory activity raises the question of possible common activity codetermining structural elements. α-Methylene-γ-lactone groups as present in the positive control, parthenolide, are a known feature but were not present in the tested compounds [70,71]. After comparison of the structures within the scope of our own results, the conjugated double bonds (as present in the most active **34**, **37**, **35**, FUR and **32**) could be hypothesized as an influencing structural element. For a conclusive statement, however, more experiments are needed due to the structural heterogeneity of the active substances. Initial evidence suggests that myrrh mediates the expression of haem oxygenase-1 and thus suppresses the inflammatory response in the in vitro model used [25]. However, there is likely more than one target in the inflammatory cascade from the stimulation by LPS to the final NO synthesis.

4. Materials and Methods

4.1. Chemicals

EtOH for extraction was purchased in technical quality from CSC Jäcklechemie (Nuremberg, Germany) and purified by evaporation. MeOH, *n*-heptane, ethyl acetate, dichloromethane, diethyl ether, and toluene (all pro analysis quality, p.a.) were obtained from Fisher Scientific (Hampton, NH, USA). Anisaldehyde (4-methoxybenzaldehyde for

synthesis), sulfuric acid (95–97%, p.a.), acetonitrile (ACN; HPLC-grade), parthenolide, and sodium nitrite (p.a.) were purchased from Merck Chemicals (Darmstadt, Germany), as well as CD_3OD from Deutero (Kastellaun, Germany), and *n*-hexane (p.a.), and chloroform-*d* (99.8%) from Sigma-Aldrich (St. Louis, MO, USA). Formic acid (p.a.) and dimethyl sulfoxide (DMSO, ≥99.5% for molecular biology) were provided by Carl Roth (Karlsruhe, Germany).

Roswell Park Memorial Institute (RPMI) 1640 medium (2 g/L $NaHCO_3$, with and without phenol red), foetal bovine serum (FBS) Superior and L-glutamine (200 mM) were purchased from Biochrom (Berlin, Germany), and 3-(4,5-dimethylthiazol-2-yl)-2,5-diphenyltetrazoliumbromide (MTT), sodium dodecyl sulfate (SDS), as well as bacterial lipopolysaccharides (LPS, from *Escherichia coli* (055:B5)) from Sigma-Aldrich (Taufkirchen, Germany). Griess reagent was prepared from 250 mg sulfanilamide (99%, Sigma-Aldrich), 25 mg N-(1-naphtyl)-ethylenediamine-dihydrochloride (≥98%, Sigma-Aldrich), 87.5 µL *o*-phosphoric acid (p.a., 85%, Merck Chemicals), and 25 mL purified water. Furanoeudesma-1,3-diene (FUR, 96%) was provided by PhytoLab (Vestenbergsgreuth, Germany).

4.2. Plant Material and Extraction

The resin of *C. myrrha* (Myrrha, Ph. Eur. 2016) was provided from Lomapharm® (lot NM0160, Rudolf Lohmann GmbH KG, Emmerthal, Germany). The powdered resin of *C. myrrha* (3 kg) was extracted by maceration and percolation with EtOH 96% (26 L) as described before [21], and 761.7 g dry extract were obtained.

4.3. Isolation

Much of the isolation process has already been published [5,21] and is therefore presented briefly and supplemented with the new methods.

4.3.1. Liquid–Liquid Partition

As a first separation step, portions of the extract were dissolved in MeOH, mixed with *n*-heptane in separatory funnels, and divided into an *n*-heptane (HEP, 70.0 g) and a MeOH soluble fraction (MeOH, 328.1 g) by liquid–liquid partition.

4.3.2. Flash Chromatography and CPC of the HEP Fraction

The second separation method used for the HEP fraction was silica flash chromatography (Spot flash system, Armen Instrument, Paris, France). The sample was partitioned into ten fractions (HEP1–10) using an SVP D40 silica column (13 × 4 cm, SI60 15–40 µm, 90 g, Götec Labortechnik GmbH, Bickenbach, Germany) with an *n*-hexane/ethyl acetate gradient. Fraction HEP7 was further separated by CPC and another silica chromatography as described earlier to gain compounds **30**, **31** [5], **32**, and **33** [21].

HEP8 (2951–3200 mL retention volume, 2.3 g weight) was then subjected to a centrifugal partition chromatography (CPC) using a Spot CPC device with a 250 mL rotor (Armen Instrument, Paris, France), a 510 HPLC pump (Waters GmbH, Eschborn, Germany), and a 2111 Multirac Fraction Collector (LKB-Produkter AB, Bromma, Sweden). The two-phase solvent system consisted of *n*-hexane, acetonitrile, and MeOH (40/25/10) [72]. The lower phase was first used as a stationary phase in ascending mode (ASC) for 800 mL; secondly, the process was continued in descending mode (DSC) for another 200 mL (flow rate 5 mL/min, rotation speed 1000 rpm). Two of the following obtained subfractions of HEP8C1–10 were further processed by preparative HPLC: fraction (mode, retention volume, and weight)—HEP8C4 (ASC 476–625 mL, 29.8 mg) and HEP8C6 (ASC 153–160 mL + DSC 15–40 mL, 154.3 mg).

4.3.3. Solid Phase Extraction and Flash Chromatography of the MeOH Fraction

To the MeOH fraction, a solid phase extraction was applied first as follows: fraction M1 (107.0 g) was eluted by ethyl acetate from the silica gel (Geduran Si 60 (0.063–0.200 mm), Merck Chemicals, Darmstadt, Germany) and fraction M2 (42.3 g) with MeOH afterwards.

As a second step, a flash chromatography was again applied to M1 using a silica column (100 × 3.6 cm, SI60 0.063–0.2 mm, approx. 520 g, Merck KGaA, Darmstadt, Germany) and a *n*-hexane/ethyl acetate/MeOH gradient. Ten subfractions M1.1–10 were collected, and fractions M1.2 (1150–1575 mL retention volume, 0.6 g weight) and M1.4 (2250–2850 mL, 7.7 g) were further processed.

4.3.4. CPC of Fraction M1.2

M1.2 was subjected to a CPC using the same conditions and two-phase solvent system as described above for HEP8. In contrast, the ASC mode was performed for 925 mL and DSC for another 275 mL. Subfractions M1.2C1–7 were formed, of which the following were processed further: fraction (mode, retention volume, and weight)—M1.2C3 (ASC 311–620 mL, 107.0 mg), M1.2C4 (ASC, 621–925 mL, 70.0 mg), M1.2C6 (DSC 986–1060 mL, 129.7 mg), and M1.2C7 (DSC, 1061–1200 mL, 73.5 mg). By preparative HPLC, M1.2C3 was processed as earlier described [5] and, additionally to the compounds presented there, **36** (18.0 min retention time; 5.6 mg weight), 1(10)*E*,4*E*-furanodienone (21.0 min; 1.9 mg), and 2-acetoxyfuranodiene (25.8 min; 1.5 mg) were gained. Furthermore, **37** was isolated from M1.2C6 and **34** and **35** from M1.2C7, as published before [5], as well as, additionally, 1*R*,2*R*-epoxy-4*S*-furanogermacr-10(14)-en-6-one (10.2 min; 5.2 mg).

4.3.5. Flash Chromatography of M1.4 and the Resulting Fraction M1.4R1F7

A dry sample of M1.4 was placed in a SVP D40 RP18 column (13 × 4 cm, RP18 25–40 µm, 90 g, Merck, Darmstadt, Germany) and separated into seven subfractions M1.4R1–7 by a water (A)/MeOH (B) gradient (0–30 min 40% A/60% B, 20 mL/min; 30–60 min 60–100% B, 20–30 mL/min; 60–90 min 100% B, 30 mL/min). After evaporation and freeze drying, M1.4R1 (90–260 mL retention volume, 1.6 g weight) was further fractionated using a FlashPure EcoFlex silica column (silica 50 µm irregular, 40 g, Büchi Labortechnik, Flawil, Switzerland) and a dichloromethane (A)/ethyl acetate (B)/MeOH (C) gradient (0–60 min 90% A/10% B–60% B, 60–80 min 40% A/60% B–100% B, 80–85 min 100% B, 85–95 min 100% B–100% C, 95–106 min 100% C) and a flow of 15 mL/min. The following four of nine subfractions were further investigated: fraction (retention volume, weight)—M1.4R1F1 (0–150 mL, 169.2 mg), M1.4R1F4 (225–330 mL, 245.0 mg), M1.4R1F6 (480–570 mL, 117.4 mg), and M1.4R1F7 (570–855 mL, 171.4 mg).

While the first three fractions were processed directly by preparative HPLC, fraction M1.4R1F7 was separated on another silica flash column (Geduran Si60 0.063–0.2 mm, 26 g, Merck, Darmstadt, Germany). An *n*-hexane (A)/ethyl acetate (B)/MeOH (C) gradient (0–25 min 60% A/40% B, 25–35 min 60% A/40% B–60% B, 35–45 min 40% A/60% B–100% B, 45–55 min 100% B, 55–65 min 100% B–100% C, 65–70 min 100% C; flow: 10 mL/min) divided it into further four subfractions M1.4R1F7.1–4, of which two were used for compound isolation as follows: fraction (retention volume, weight)—M1.4R1F7.1 (145–430 mL, 43.7 mg) and M1.4R1F7.2 (430–490 mL, 24.4 mg).

4.3.6. Thin-Layer Chromatography (TLC)

TLC analysis of the fractions of CPC and flash chromatographic separations was conducted on silica gel 60 F254 (Merck, Darmstadt, Germany) with mobile phases consisting of toluene/ethyl acetate 95/5 or 80/20 (*v*/*v*) for the HEP fractions and the fractions gained from M1.2, *n*-hexane/ethyl acetate/MeOH 15/80/5 (*v*/*v*/*v*) for the MeOH fractions or *n*-hexane/ethyl acetate/formic acid 2/3/0.1 (*v*/*v*/*v*) for the fractions gained from M1.4. Compounds were derivatized by anisaldehyde reagent *R* (Ph. Eur.) and detected as well as documented by a Camag TLC visualizer (Camag AG, Muttenz, Switzerland).

4.3.7. Preparative HPLC

For final substance isolation, a preparative HPLC device including a 1260 Infinity binary pump, a 1260 Infinity manual injector, a 1260 Infinity fraction collector, a 1260 Infinity diode array detector (all Agilent Technologies, Santa Clara, CA, USA), and a Kinetex®

column (Biphenyl, 100 Å, 5 µm, 21.2 × 250 mm, Phenomenex, Aschaffenburg, Germany; 21 mL/min flow rate) were used; only for M1.2C4, a Nucleodur^{TM} C18 Isis column was used (RP18, 5 µm, 10 × 250 mm, Macherey-Nagel, Düren, Germany; 5 mL/min flow rate). The compounds were separated by ACN/water gradients (Table 8) and detected at 200 nm. Afterwards, the ACN was eliminated by evaporation, the aqueous phases partitioned four times with diethyl ether and the organic phases were dried under a nitrogen stream.

Table 8. Water/ACN gradients for the separation of the respective fractions on a biphenyl column (M1.2C4: Nucleodur C18 column) and retention times of the isolated compounds.

Fraction	Gradient		Retention Time [min], Compound No.
	Time [min]	ACN [%]	
HEP8C4	0 11 11.1 13	70 87 100 100	7.5, **38**; 9.5, **42**; 9.8, **40**; 10.2, **39**
HEP8C6	0 20 25	60 100 100	19.7 min, **41**
M1.2C4	0 15 16 25	55 75 100 100	10.5, **29**; 12.0 min, curzerenone (2.1 mg); 15.0 min, myrrhone (6.4 mg)
M1.4R1F1	0 15 20 25	30 40 90 90	9.5, **16**; 10.0, **10**; 12.3, mixture of **3**, **4** and **22**; 15.0, **26**; 20.8, **43**
M1.4R1F4	0 20 21 26	20 32 90 90	11.6, **12**; 12.0, **24**; 13.6, **11**; 14.0, **23**; 15.9, **15**; 17.3, **5**; 17.6, **27**; 18.1, **2**; 20.5, **8**; 21.4, **6**; 22.1, mixture of **18** and **20**
M1.4R1F6	0 15 16 21	20 30 90 90	12.4, **7**; 13.2 **13**; 15.5, **17**
M1.4R1F7.2			4.9, **1**, 6.6, **14**; 14.4, **9**
M1.4R1F7.1	0 25 26 31	17 23 95 95	24.4, (–)-**21**; 25.2, **25**; 25.6, **19**; 28.0, **28**

4.4. Compound Characterisation

The 1D and 2D NMR spectra (^{1}H, ^{13}C, HSQC, HMBC, COSY and NOESY) were recorded at 298 K in CD_3OD or $CDCl_3$ on an AVANCE III 600 NMR equipped with a 5 mm TBI CryoProbe or an AVANCE III HD 400 NMR (Bruker Corporation, Billerica, MA, USA).

HRESIMS analysis of the isolates was performed with a 1290 Infinity UHPLC as well as a ZORBAX Eclipse column (XDB-C18 RRHD, 2.1 × 100 mm, 1.8 µm; Agilent Technologies, Santa Clara, CA, USA). The solvent system consisted of 0.1% formic acid in water or in ACN, and electrospray ionization (ESI) was carried out in the positive and negative modes. For the triterpenoid and phytosteroid compounds, GC combined with chemical ionisation (APCI) were chosen to achieve their sufficient ionisation. An Agilent 7890A GC system and a (5% phenyl)-methylpolysiloxane phase capillary column Agilent 19091S-433HP-5MS (30 m, 0.25 mm, 0.25 µm, 7-inch cage) were used (Agilent Technologies). For both separation modes, LC and GC, the ionisation and mass spectrometric analysis were conducted using a Q-TOF 6540 UHD mass spectrometer (Agilent Technologies).

Optical properties of all compounds were measured using solutions in MeOH. The specific optical rotation at 589 nm was obtained using an UniPol L 1000 polarimeter (Schmidt + Haensch GmbH & Co., Berlin, Germany). A Cary 50 Scan UV–Vis spectrophotometer (Varian Deutschland GmbH, Darmstadt, Germany) was applied for recording UV–Vis spectra in a range of 200–800 nm. Additionally, CD spectra were measured on a J-715 spectropolarimeter (JASCO Deutschland GmbH, Gross-Umstadt, Germany) with a 0.1 cm quartz cuvette. Thereby, ten scans from 190–300 or 350 nm (scanning rate: 100 nm/min; 0.5 nm steps; 22 °C) were averaged and smoothed by the Savitzky–Golay algorithm (convolution width: 15).

The purity of the isolates was determined by HPLC-DAD analysis on an Elite LaChrom system consisting of an autosampler L-2200, a pump L-2130, a column oven L-2350, a DAD L-2455 (all Hitachi, Tokyo, Japan) and a Kinetex® biphenyl column (100 Å, 5 µm, 4.6 × 250 mm, Phenomenex, Aschaffenburg, Germany), or a Nucleodur™ C18 Isis column (RP18, 5 µm, 4.6 × 250 mm, Macherey-Nagel, Düren, Germany), respectively. The respective gradients used for isolation (Table 8) were conducted at a flow rate of 1 mL/min. The purity was calculated as the proportion of the integral of the main peak in the chromatogram in the maxplot (190–400 nm for the HEP fraction or 200–400 nm for the MeOH fraction) using the software EZChrom Elite 3.1.7 (Hitachi, Tokyo, Japan).

4.5. Isolated Compounds

The following chemical structures were drawn in ChemDrawProfessional 20.0, and three-dimensional models were generated with Chem3D Ultra 20.0 (both PerkinElmer Informatics Inc., Waltham, MA, USA).

1β,5,8-Trihydroxy-4α,8-cycloeudesma-2,7(11)Z-dien-12-al (**1**): 1.4 mg, colourless oil; $[\alpha]_D^{25}$ −226 (*c* 1.17, MeOH); UV (MeOH) λ_{max} (log ε): 257 nm (3.92); CD: Figure S24; ^{1}H and ^{13}C NMR data: Table 1, original spectra: Figure S1, HSQC and HMBC: Figure S2, COSY and NOESY: Figure S3; HRESIMS *m*/*z* 265.1435 $[M+H]^+$ (calc. for $C_{15}H_{21}O_4$, 265.1434); purity: 92.1%.

2β-Acetyloxy-6β-hydroxyglechomanolide (**2**): 2.5 mg, colourless oil; $[\alpha]_D^{22}$ −15 (*c* 2.51, MeOH); UV (MeOH) λ_{max} (log ε): 208 nm (4.06); CD: Figure S24; ^{1}H and ^{13}C NMR data: Table 1, original spectra: Figure S4; HRESIMS *m*/*z* 307.1545 $[M+H]^+$ (calc. for $C_{17}H_{23}O_5$, 307.1540); purity: 87.6%.

4β,5α-Epoxyglechomanolide (**3**): in mixture with **4** and **22**: 13.1 mg, yellowish oil; ^{1}H and ^{13}C NMR data: Table 1, original spectra: Figure S5; HRESIMS *m*/*z* 249.1485 $[M+H]^+$ (calc. for $C_{15}H_{21}O_3$, 249.1491).

2β-Acetyloxy-4β,5α-epoxyglechomanolide (**4**): in mixture with **3** and **22**: 13.1 mg, yellowish oil; ^{1}H and ^{13}C NMR data: Table 1, original spectra: Figure S6; HRESIMS *m*/*z* 307.1543 $[M+H]^+$ (calc. for $C_{17}H_{23}O_5$, 307.1545).

2β-Acetyloxy-4β,5α-epoxy-8-epi-*hydroxyglechomanolide* (**5**): 5.2 mg, white solid; $[\alpha]_D^{23}$ +17 (*c* 2.61, MeOH); UV (MeOH) λ_{max} (log ε): no maximum detected; CD: Figure S24; ^{1}H and ^{13}C NMR data: Table 2, original spectra: Figure S7; HRESIMS *m*/*z* 323.1492 $[M+H]^+$ (calc. for $C_{17}H_{23}O_6$, 323.1489); purity: 88.7%.

8-epi-*Serralactone A* (**6**): 4.3 mg, colourless oil; $[\alpha]_D^{23}$ −2.0 (*c* 2.13, MeOH); UV (MeOH) λ_{max} (log ε): 219 nm (4.10); CD: Figure S24; ^{1}H and ^{13}C NMR data: Table 2, original spectra: Figure S8; HRESIMS *m*/*z* 249.1491 $[M+H]^+$ (calc. for $C_{15}H_{21}O_3$, 249.1485); purity: 93.2%.

1α,8β-Dihydroxy-2β-ethyloxyeudesma-3,7(11)-dien-8α,12-olide (**7**): 2.6 mg, colourless oil; $[\alpha]_D^{23}$ +5.8 (*c* 2.36, MeOH); UV (MeOH) λ_{max} (log ε): no maximum detected; CD: Figure S24; ^{1}H and ^{13}C NMR data: Table 2, original spectra: Figure S9; HRESIMS *m*/*z* 309.1698 $[M+H]^+$ (calc. for $C_{17}H_{25}O_5$, 309.1697); purity: 81.9%.

8-epi-*Neolitacumone B* (**8**): 1.8 mg, yellowish oil; $[\alpha]_D^{22}$ +43 (*c* 1.81, MeOH); UV (MeOH) λ_{max} (log ε): 221 nm (3.99), 276 nm (3.34); CD: Figure S24; ^{1}H and ^{13}C NMR data: Table 3, original spectra: Figure S10; HRESIMS *m*/*z* 249.1490 $[M+H]^+$ (calc. for $C_{15}H_{21}O_3$, 249.1491); purity: 76.7%.

2α-Acetyloxyneolitacumone A (**9**): 1.6 mg, white solid; $[\alpha]_D^{25}$ −89 (*c* 1.57, MeOH); UV (MeOH) λ_{max} (log ε): 214 nm (3.96); CD: Figure S24; ^{1}H and ^{13}C NMR data: Table 3, original spectra: Figure S11; HRESIMS *m*/*z* 321.1344 $[M–H]^-$ (calc. for $C_{17}H_{21}O_6$, 321.1344); purity: 84.0%.

*3-Oxo-8α*H-*eudesma-1,4,7(11)-trien-8,12-olide* (**10**): 2.5 mg, yellowish oil; $[\alpha]_D^{23}$ −37 (*c* 2.05, MeOH); UV (MeOH) λ_{max} (log ε): 221 nm (3.87); CD: Figure S24; ^{1}H and ^{13}C NMR data: Table 3, original spectra: Figure S12; HRESIMS *m*/*z* 245.1174 $[M+H]^+$ (calc. for $C_{15}H_{17}O_3$, 245.1172); purity: 93.0%.

*3-Oxo-8β-hydroxy-5α*H-*eudesma-1,4(15),7(11)-trien-8,12-olide* (**11**): 2.1 mg, colourless oil; $[\alpha]_D^{24}$ −18 (*c* 2.08, MeOH); UV (MeOH) λ_{max} (log ε): 220 nm (4.06); CD: Figure S24; ^{1}H and ^{13}C NMR data: Table 3, original spectra: Figure S13; HRESIMS *m*/*z* 261.1126 $[M+H]^+$ (calc. for $C_{15}H_{17}O_4$, 261.1121); purity: 86.2%.

4-epi-*Linderolide J* (**12**): 1.8 mg, yellowish oil; $[\alpha]_D^{23}$ +71 (*c* 1.82, MeOH); UV (MeOH) λ_{max} (log ε): 221 nm (3.88); CD: Figure S24; ^{1}H and ^{13}C NMR data: Table 4, original spectra: Figure S14; HRESIMS *m*/*z* 277.1067 $[M+H]^+$ (calc. for $C_{15}H_{17}O_5$, 277.1071); purity: 87.4%.

*1β,8β-Dihydroxy-5α*H-*eudesma-2,4(15),7(11)-trien-8,12-olide* (**13**): 1.8 mg, white solid; $[\alpha]_D^{23}$ +33 (*c* 1.78, MeOH); UV (MeOH) λ_{max} (log ε): 223 nm (3.93); CD: Figure S24; ^{1}H and ^{13}C NMR data: Table 4, original spectra: Figure S15; HRESIMS *m*/*z* 263.1277 $[M+H]^+$ (calc. for $C_{15}H_{19}O_4$, 263.1278); purity: 95.5%.

1α,5α,8β-Trihydroxyeudesma-2,4(15),7(11)-trien-8,12-olide (**14**): 0.8 mg, white solid; $[\alpha]_D^{25}$ +146 (*c* 0.87, MeOH); UV (MeOH) λ_{max} (log ε): 223 nm (3.98); CD: Figure S24; ^{1}H and ^{13}C NMR data: Table 4, original spectra: Figure S16; HRESIMS *m*/*z* 279.1226 $[M+H]^+$ (calc. for $C_{15}H_{19}O_5$, 279.1227); purity: 93.0%.

1α,5α-Dihydroxyeudesma-2,4(15),7(11),8-tetraen-8,12-olide (**15**): 5.0 mg, yellowish oil; $[\alpha]_D^{24}$ +168 (*c* 2.49, MeOH); UV (MeOH) λ_{max} (log ε): 224 nm (4.02), 276 nm (3.96); CD: Figure S24; ^{1}H and ^{13}C NMR data: Table 5, original spectra: Figure S17; HRESIMS *m*/*z* 261.1125 $[M+H]^+$ (calc. for $C_{15}H_{17}O_4$, 261.1121); purity: 87.3%.

1,2-Anhydro-8-oxo-tussfarfarin A (**16**): 4.7 mg, yellowish oil; $[\alpha]_D^{23}$ +75 (*c* 2.04, MeOH); UV (MeOH) λ_{max} (log ε): 318 nm (3.81); CD: Figure S24; ^{1}H and ^{13}C NMR data: Table 5, original spectra: Figure S18; HRESIMS *m*/*z* 231.1017 $[M+H]^+$ (calc. for $C_{14}H_{15}O_3$, 231.1016); purity: 98.3%.

8,14-Dihydroxy-9,10-seco-isolindestrenolide (**17**): 1.0 mg, white solid; $[\alpha]_D^{23}$ −9.5 (*c* 0.99, MeOH); UV (MeOH) λ_{max} (log ε): shoulder at 275 nm; CD: Figure S24; ^{1}H and ^{13}C NMR data: Table 5, original spectra: Figure S19; HRESIMS *m*/*z* 263.1274 $[M+H]^+$ (calc. for $C_{15}H_{19}O_4$, 263.1278); purity: 94.0%.

Serralactone A (**18**): in mixture with **20**: 6.6 mg, white solid; ^{1}H and ^{13}C NMR data: comparable to [26]; HRESIMS *m*/*z* 249.1491 $[M+H]^+$ (calc. for $C_{15}H_{21}O_3$, 249.1491).

1β,8β-Dihydroxyeudesman-3,7(11)-dien-8α,12-olide (**19**): 5.0 mg, white solid; $[\alpha]_D^{25}$ −9.7 (*c* 2.19, MeOH); UV (MeOH) λ_{max} (log ε): 214 nm (3.99); CD: Figure S25; ^{1}H and ^{13}C NMR data: comparable to [27]; HRESIMS *m*/*z* 265.1437 $[M+H]^+$ (calc. for $C_{15}H_{21}O_4$, 265.1434); purity: 82.5%.

Neolitacumone B (**20**): in mixture with **18**: 6.6 mg, white solid; ^{1}H and ^{13}C NMR data: comparable to [28]; HRESIMS *m*/*z* 249.1491 $[M+H]^+$ (calc. for $C_{15}H_{21}O_3$, 249.1491).

(–)-Neolitacumone A ((–)-**21**): 3.6 mg, white solid; $[\alpha]_D^{25}$ −7.3 (*c* 2.02, MeOH); UV (MeOH) λ_{max} (log ε): 220 nm (3.96); CD: Figure S25; ^{1}H and ^{13}C NMR data: comparable to [28]; HRESIMS *m*/*z* 265.1438 $[M+H]^+$ (calc. for $C_{15}H_{21}O_4$, 265.1434); purity: 94.1%.

*3-Oxo-5α*H,*8β*H-*eudesma-1,4(15),7(11)-trien-8,12-olide* (**22**): in mixture with **3** and **4**: 13.1 mg, yellowish oil; ^{1}H and ^{13}C NMR data: comparable to [29]; HRESIMS *m*/*z* 245.1176 $[M+H]^+$ (calc. for $C_{15}H_{17}O_3$, 245.1172).

(+)-Eudebeiolide B (**23**): 1.6 mg, colourless oil; $[\alpha]_D^{24}$ +46 (*c* 1.58, MeOH); UV (MeOH) λ_{max} (log ε): 220 nm (4.03); CD: Figure S25, determination of the absolute configuration in comparison to [30]; ^{1}H and ^{13}C NMR data: comparable to [30]; HRESIMS *m*/*z* 263.1280 $[M+H]^+$ (calc. for $C_{15}H_{19}O_4$, 263,1278); purity: 70.2%.

Linderolide I (**24**): 2.7 mg, yellowish oil; $[\alpha]_D^{23}$ +82 (*c* 2.72, MeOH); UV (MeOH) λ_{max} (log ε): 221 nm (4.07), shoulder at 275 nm; CD: Figure S25; ^{1}H and ^{13}C NMR data: Table 5; HRESIMS *m*/*z* 263.1281 $[M+H]^+$ (calc. for $C_{15}H_{19}O_4$, 263.1278); purity: 92.3%.

1β,8β-Dihydroxyeudesma-4,7(11)-dien-8α,12-olide (**25**): 1.8 mg, white solid; $[\alpha]_D^{25}$ −19 (*c* 0.92, MeOH); UV (MeOH) λ_{max} (log ε): 218 nm (4.00); CD: Figure S25; ^{1}H and ^{13}C NMR data: comparable to [73]; HRESIMS *m*/*z* 265.1438 $[M+H]^+$ (calc. for $C_{15}H_{21}O_4$, 265.1434); purity: 78.6%.

Istanbulin B (**26**): 6.4 mg, yellowish oil; $[\alpha]_D^{23}$ −5.4 (*c* 2.12, MeOH); UV (MeOH) λ_{max} (log ε): 220 nm (4.14); CD: Figure S25; ^{1}H and ^{13}C NMR data: comparable to [74]; HRESIMS *m*/*z* 249.1490 $[M+H]^+$ (calc. for $C_{15}H_{21}O_3$, 249.1491); purity: 94.8%.

Istanbulin A (**27**): 4.0 mg, white solid; $[\alpha]_D^{24}$ +23 (*c* 2.47, MeOH); UV (MeOH) λ_{max} (log ε): 219 nm (3.93); CD: Figure S25; ^{1}H and ^{13}C NMR data: comparable to [74]; HRESIMS *m*/*z* 265.1436 $[M+H]^+$ (calc. for $C_{15}H_{21}O_4$, 265.1434); purity: 70.3%.

Chloraniolide A (**28**): 2.3 mg, yellowish oil; $[\alpha]_D^{25}$ −4.2 (*c* 2.33, MeOH); UV (MeOH) λ_{max} (log ε): shoulder at 218 nm; CD: Figure S25; ^{1}H and ^{13}C NMR data: comparable to [34]; HRESIMS *m*/*z* 267.1595 $[M+H]^+$ (calc. for $C_{15}H_{23}O_4$, 267.1591); purity: 65.2%.

*2S-Methoxy-4S-furanogermacra-1(10)*E*-en-6-one* (**29**): 11.6 mg, white solid; $[\alpha]_D^{22}$ −89 (*c* 2.58, MeOH); UV (MeOH) λ_{max} (log ε): 206 nm (3.98); CD: Figure S25, determination of the absolute configuration in comparison to [38]; ^{1}H and ^{13}C NMR data: comparable to [37]; HRESIMS *m*/*z* 263.1640 $[M]^+$ (calc. for $C_{16}H_{23}O_3$, 263.1642) purity: 91.2%.

The physicochemical properties of compounds **30**, **31**, **34**, **35** and **37** [5] as well as **32** and **33** [21] were published before.

Alismol (**36**): 5.6 mg, colourless oil; $[\alpha]_D^{22}$ −0.8 (*c* 2.1, MeOH); UV (MeOH) λ_{max} (log ε): no maximum detected; CD: Figure S25; ^{1}H and ^{13}C NMR data: comparable to [75]; HRESIMS *m*/*z* 220.1816 $[M]^+$ (calc. for $C_{15}H_{24}O$; 220.1827); purity: 90.5%.

29-Norlanost-8,24-dien-1α,3β-diol (**38**): 2.4 mg, white solid; $[\alpha]_D^{22}$ +93 (*c* 2.40, MeOH); UV (MeOH) λ_{max} (log ε): 203 nm (4.10); CD: Figure S25; ^{1}H and ^{13}C NMR data: Table 6, original spectra: Figure S20; GC-APCI *m*/*z* 429.3727 $[M+H]^+$ (calc. for $C_{29}H_{49}O_2$, 429.3727); purity: 84.8%.

11α-Hydroxysitost-4-en-3-one (**39**): 0.8 mg, colourless oil; $[\alpha]_D^{23}$ +40 (*c* 0.89, MeOH); UV (MeOH) λ_{max} (log ε): 203 nm (3.96); CD: Figure S25; ^{1}H and ^{13}C NMR data: Table 6, original spectra: Figure S21; GC-APCI *m*/*z* 429.3728 $[M+H]^+$ (calc. for $C_{29}H_{49}O_2$, 429.3727); purity: 83.5%.

11α-Hydroxystigmast-4-en-3-one (**40**): 0.4 mg, white solid; $[\alpha]_D^{22}$ +39 (*c* 0.44, MeOH); UV (MeOH) λ_{max} (log ε): 243 nm (4.36); CD: Figure S25; ^{1}H and ^{13}C NMR data: Table 6, original spectra: Figure S22; GC-APCI *m*/*z* 427.3570 $[M+H]^+$ (calc. for $C_{29}H_{47}O_2$, 427.3571); purity: 87.5%.

*Stigmasta-5,22*E*-diene-3β,11α-diol* (**41**): 4.7 mg, yellowish solid; $[\alpha]_D^{23}$ −2.9 (*c* 2.35, MeOH); UV (MeOH) λ_{max} (log ε): 201 nm (3.96); CD: Figure S25; ^{1}H and ^{13}C NMR data comparable to [36]; GC-APCI *m*/*z* 446.3988 $[M+NH_4]^+$ (calc. for $C_{29}H_{49}NO_2$, 446.3993); purity: 45.1%.

7-Ketostigmasterol (**42**): 0.5 mg, white solid; $[\alpha]_D^{22}$ −21 (*c* 0.56, MeOH); UV (MeOH) λ_{max} (log ε): 238 nm (4.03); CD: Figure S26; ^{1}H and ^{13}C NMR data: comparable to [76]; GC-APCI *m*/*z* 427.3572 $[M+H]^+$ (calc. for $C_{29}H_{47}O_2$, 427.3571); purity: 84.1%.

rel-*7′-(3′-Methoxy-4′,5′-methylendioxyphenyl)-3,4,5-trimethoxy-7,8*S*,7′*R*,8′*R*-tetrahydronaphtho[2,3-c]furan-9′(3H)-one* (**43**): 1.3 mg, yellowish solid; $[\alpha]_D^{24}$ −1.7 (*c* 1.26, MeOH); UV (MeOH) λ_{max} (log ε): shoulder at approx. 280 nm; CD: Figure S26; ^{1}H and ^{13}C NMR data: Table 7, original spectra: Figure S23; HRESIMS *m*/*z* 429.1547 $[M+H]^+$ (calc. for $C_{23}H_{25}O_8$, 429.1544); purity: 42.3%.

4.6. RAW 264.7 Experiments

The RAW 264.7 mouse macrophages cell line was purchased from CLS (Eppelheim, Germany). The cells were cultured in RPMI 1640 medium with phenol red, supplemented

with 10% heat inactivated FBS and 1% L-glutamine, as well as in an atmosphere of 5% CO_2 and 90% relative humidity at 37 °C. Mycoplasma contamination was excluded by PCR and culture from GATC Biotech AG (Konstanz, Germany).

4.6.1. MTT Assay

This assay was performed similarly as previously described [5,77]. Cells from a confluent culture flask were seeded into 96-well plates in RPMI medium without phenol red (10,000 cells/well in 100 µL) and incubated for 24 h. The medium was then removed, a sample solution in medium was added (5–100 µM, max. 0.14% DMSO, *v*/*v*), and the cells were incubated for a further 24 h. Subsequently, the supernatant was replaced with 100 µL of an MTT solution in medium (0.4 mg/mL) and incubated for three hours. The cells were then treated with 10% SDS in water and stored at room temperature in the dark. By the next day, the formazan crystals had dissolved and the absorbance at 560 nm could be determined using a Tecan microplate reader (Tecan Trading AG, Maennedorf, Switzerland). Cell viability was calculated as a proportion compared to the average absorbance of the negative control (medium only). To exclude the possibility of solvent effects, some cells were also treated with the highest DMSO concentration used. All assays were performed three times independently in hexaplicates.

4.6.2. Griess Assay

Cells from a confluent culture flask were seeded into 96-well plates in RPMI medium without phenol red (100,000 cells/well in 100 µL) and incubated for 24 h. The medium was then removed, a sample solution in medium containing 1 µg/mL LPS was added (1–70 µM, max. 0.1% DMSO, *v*/*v*), and the cells were incubated for a further 24 h. A total of 70 µL of the supernatants were then mixed with the same volume of Griess reagent under exclusion of light and, after 15 min, the absorbance at 560 nm was measured using a Tecan microplate reader (Tecan Trading AG, Maennedorf, Switzerland). Nitrite concentrations were determined by an external calibration with sodium nitrite, and their proportions to the negative control were calculated. Parthenolide (5 µM) was used as a positive control, medium without LPS as an untreated control, medium with LPS as a negative control, and the highest DMSO concentration used as a solvent control. All assays were performed three times independently in hexaplicates.

4.6.3. Statistics

Significance levels were calculated in two-sided Student's *t*-tests using Microsoft Excel 2305 (Microsoft Corporation, Redmond, WA, USA). The diagrams were made by GraphPad Prism 5.00 (GraphPad Software, Boston, MA, USA), which was also used to determine the nonlinear regression curve.

Supplementary Materials: The following supporting information can be downloaded at: https://www.mdpi.com/article/10.3390/molecules29184315/s1, Figure S1. ^{1}H (600 MHz) and ^{13}C NMR (151 MHz) spectrum of compound **1** in CD_3OD. Figure S2. HSQC and HMBC spectrum of compound **1** in CD_3OD. Figure S3. COSY and NOESY spectrum of compound **1** in CD_3OD. Figures S4–S23: ^{1}H and ^{13}C NMR spectra of compounds **2**–**17**, **38**–**40** and **43**. Figure S24. CD spectra of compounds **1**, **2**, **5**–**17** in MeOH, [θ] in [(°cm^2) × dmol^{-1}]. Figure S25**.** CD spectra of **19**, (-)-**21**, **23**–**29**, **36** and **38**–**41** in MeOH, [θ] in [(°cm^2) × dmol^{-1}]. Figure S26. CD spectra of compounds **42** and **43** in MeOH, [θ] in [(°cm^2) × dmol^{-1}]. Figure S27. Influence of compounds **1**, (–)-**21**, **29**–**37** and furanoeudesma-1,3-diene (FUR) on the viability of RAW 264.7 cells in the MTT assay. The test was performed including a negative control (n.c., medium only) and two solvent controls (s.c. 1: 0.1% DMSO, s.c. 2: 0.14% DMSO, *v*/*v*). Data are presented as mean ± SEM, * $p < 0.05$ vs. n.c. (student's *t*-test, $n = 3$). Figures S28–S37. ^{1}H and ^{13}C NMR spectra of compounds **21** and **29**–**37** and **43**.

Author Contributions: Conceptualization, J.H.; methodology, formal analysis, and investigation: A.U., K.K., and A.W.; resources, J.H.; writing—original draft preparation, A.U.; writing—review and editing, K.K., J.H., and B.L.; visualization, A.U.; supervision, J.H. and B.L.; project administration,

J.H.; funding acquisition, J.H. All authors have read and agreed to the published version of the manuscript.

Funding: This research was funded by Repha GmbH Biologische Arzneimittel. The APC was funded by the publication fund of University of Regensburg.

Institutional Review Board Statement: Not applicable.

Informed Consent Statement: Not applicable.

Data Availability Statement: The data presented in this study are available on request from J.H. and A.U.

Acknowledgments: The authors gratefully acknowledge Repha GmbH Biologische Arzneimittel for scientific discussions and financial support. Fritz Kastner and Tuan-Anh Nguyen are kindly acknowledged for performing the 1D and 2D NMR experiments, as are Josef Kiermaier and Wolfgang Söllner for acquiring the MS data (all: Zentrale Analytik, Faculty of Chemistry and Pharmacy, University of Regensburg). Furthermore, thanks are due to Thomas Gruber for the photo of myrrh depicted in the graphical abstract.

Conflicts of Interest: B.L. is employed by Repha GmbH Biologische Arzneimittel. All other authors (A.U., K.K., A.W. and J.H.) declare no conflicts of interest.

References

1. Mahr, D. *Commiphora*: An introduction to the genus. *Cactus Succul. J.* **2012**, *84*, 140–154. [CrossRef]
2. Tucker, A.O. Frankincense and myrrh. *Econ. Bot.* **1986**, *40*, 425–433. [CrossRef]
3. Hanuš, L.O.; Řezanka, T.; Dembitsky, V.M.; Moussaieff, A. Myrrh-*Commiphora* chemistry. *Biomed. Pap.* **2005**, *149*, 3–28. [CrossRef] [PubMed]
4. Liu, J.-W.; Zhang, M.-Y.; Yan, Y.-M.; Wei, X.-Y.; Dong, L.; Zhu, Y.-X.; Cheng, Y.-X. Characterization of sesquiterpene dimers from *Resina Commiphora* that promote adipose-derived stem cell proliferation and differentiation. *J. Org. Chem.* **2018**, *83*, 2725–2733. [CrossRef] [PubMed]
5. Kuck, K.; Unterholzner, A.; Lipowicz, B.; Schwindl, S.; Jürgenliemk, G.; Schmidt, T.J.; Heilmann, J. Terpenoids from myrrh and their cytotoxic activity against HeLa cells. *Molecules* **2023**, *28*, 1637. [CrossRef]
6. Wang, C.-C.; Liang, N.-Y.; Xia, H.; Wang, R.-Y.; Zhang, Y.-F.; Huo, H.-X.; Zhao, Y.-F.; Song, Y.-L.; Zheng, J.; Tu, P.-F. Cytotoxic sesquiterpenoid dimers from the resin of *Commiphora myrrha* Engl. *Phytochemistry* **2022**, *204*, 113443. [CrossRef]
7. Ge, C.-Y.; Zhang, J.-L. Bioactive sesquiterpenoids and steroids from the resinous exudates of *Commiphora myrrha*. *Nat. Prod. Res.* **2019**, *33*, 309–315. [CrossRef]
8. El-Razek, A.; Mohamed, T.A.; Abdel-Halim, S.; Bata, S.M.; Kubacy, T.M. Comprehensive NMR reassignments of lignans derived from *Commiphora myrrha*. *Egypt. J. Chem.* **2023**, *66*, 45–57. [CrossRef]
9. Shen, T.; Li, G.-H.; Wang, X.-N.; Lou, H.-X. The genus *Commiphora*: A review of its traditional uses, phytochemistry and pharmacology. *J. Ethnopharmacol.* **2012**, *142*, 319–330. [CrossRef]
10. Tariq, M.; Ageel, A.M.; Al-Yahya, M.A.; Mossa, J.S.; Al-Said, M.S.; Parmar, N.S. Anti-inflammatory activity of *Commiphora molmol*. *Agents Actions* **1985**, *17*, 381–382. [CrossRef]
11. Su, S.; Duan, J.; Chen, T.; Huang, X.; Shang, E.; Yu, L.; Wei, K.; Zhu, Y.; Guo, J.; Guo, S.; et al. Frankincense and myrrh suppress inflammation via regulation of the metabolic profiling and the MAPK signaling pathway. *Sci. Rep.* **2015**, *5*, 13668. [CrossRef] [PubMed]
12. Hamad, G.M.; Taha, T.H.; Alshehri, A.; El-Deeb, N.M. Myrrh as a functional food with therapeutic properties against colon cancer in traditional meals. *J. Food Process. Preserv.* **2017**, *41*, e12963. [CrossRef]
13. Rahman, M.M.; Garvey, M.; Piddock, L.J.V.; Gibbons, S. Antibacterial terpenes from the oleo-resin of *Commiphora molmol* (Engl.). *Phytother. Res.* **2008**, *22*, 1356–1360. [CrossRef] [PubMed]
14. Alhussaini, M.S.; Saadabi, A.M.; Mohammed, I. Alghonaim; Khalid Elfakki Ibrahim. An evaluation of the antimicrobial activity of *Commiphora myrrha* Nees (Engl.) oleo-gum resins from Saudi Arabia. *J. Med. Sci.* **2015**, *15*, 198–203. [CrossRef]
15. Dolara, P.; Luceri, C.; Ghelardini, C.; Monserrat, C.; Aiolli, S.; Luceri, F.; Lodovici, M.; Menichetti, S.; Romanelli, M.N. Analgesic effects of myrrh. *Nature* **1996**, *379*, 29. [CrossRef]
16. Germano, A.; Occhipinti, A.; Barbero, F.; Maffei, M.E. A pilot study on bioactive constituents and analgesic effects of MyrLiq®, a *Commiphora myrrha* extract with a high furanodiene content. *BioMed Res. Int.* **2017**, *2017*, 3804356. [CrossRef]
17. Fatani, A.J.; Alrojayee, F.S.; Parmar, M.Y.; Abuohashish, H.M.; Ahmed, M.M.; Al-Rejaie, S.S. Myrrh attenuates oxidative and inflammatory processes in acetic acid-induced ulcerative colitis. *Exp. Ther. Med.* **2016**, *12*, 730–738. [CrossRef]
18. Langhorst, J.; Varnhagen, I.; Schneider, S.B.; Albrecht, U.; Rueffer, A.; Stange, R.; Michalsen, A.; Dobos, G.J. Randomised clinical trial: A herbal preparation of myrrh, chamomile and coffee charcoal compared with mesalazine in maintaining remission in ulcerative colitis—A double-blind, double-dummy study. *Aliment. Pharmacol. Ther.* **2013**, *38*, 490–500. [CrossRef]

19. Fraternale, D.; Sosa, S.; Ricci, D.; Genovese, S.; Messina, F.; Tomasini, S.; Montanari, F.; Marcotullio, M.C. Anti-inflammatory, antioxidant and antifungal furanosesquiterpenoids isolated from *Commiphora erythraea* (Ehrenb.) Engl. resin. *Fitoterapia* **2011**, *82*, 654–661. [CrossRef]
20. Messina, F.; Gigliarelli, G.; Palmier, A.; C Marcotullio, M. Furanodienone: An emerging bioactive furanosesquiterpenoid. *Curr. Org. Chem.* **2017**, *21*, 305–310. [CrossRef]
21. Kuck, K.; Jürgenliemk, G.; Lipowicz, B.; Heilmann, J. Sesquiterpenes from myrrh and their ICAM-1 inhibitory activity in vitro. *Molecules* **2020**, *26*, 42. [CrossRef] [PubMed]
22. Cao, B.; Wei, X.-C.; Xu, X.-R.; Zhang, H.-Z.; Luo, C.-H.; Feng, B.; Xu, R.-C.; Zhao, S.-Y.; Du, X.-J.; Han, L.; et al. Seeing the unseen of the combination of two natural resins, frankincense and myrrh: Changes in chemical constituents and pharmacological activities. *Molecules* **2019**, *24*, 3076. [CrossRef] [PubMed]
23. Bogdan, C. Nitric oxide and the immune response. *Nat. Immunol.* **2001**, *2*, 907–916. [CrossRef] [PubMed]
24. Boughton-Smith, N.K.; Evans, S.M.; Whittle, B.J.; Moncada, S.; Hawkey, C.J.; Cole, A.T.; Balsitis, M. Nitric oxide synthase activity in ulcerative colitis and Crohn's disease. *Lancet* **1993**, *342*, 338-e2. [CrossRef] [PubMed]
25. Cheng, Y.-W.; Cheah, K.-P.; Lin, C.-W.; Li, J.-S.; Yu, W.-Y.; Chang, M.L.; Yeh, G.-C.; Chen, S.-H.; Choy, C.-S.; Hu, C.-M. Myrrh mediates haem oxygenase-1 expression to suppress the lipopolysaccharide-induced inflammatory response in RAW264.7 macrophages. *J. Pharm. Pharmacol.* **2011**, *63*, 1211–1218. [CrossRef]
26. Teng, F.; Zhong, H.-M.; Chen, C.-X.; Liu, H.-Y. Four new eudesmane sesquiterpenoid lactones from *Chloranthus serratus*. *HCA* **2009**, *92*, 1298–1303. [CrossRef]
27. El-Gamal, A.A. Sesquiterpene lactones from *Smyrnium olusatrum*. *Phytochemistry* **2001**, *57*, 1197–1200. [CrossRef]
28. Chang, F.-R.; Hsieh, T.-J.; Huang, T.-L.; Chen, C.-Y.; Kuo, R.-Y.; Chang, Y.-C.; Chiu, H.-F.; Wu, Y.-C. Cytotoxic constituents of the stem bark of *Neolitsea acuminatissima*. *J. Nat. Prod.* **2002**, *65*, 255–258. [CrossRef]
29. Ohno, T.; Nagatsu, A.; Nakagawa, M.; Inoue, M.; Li, Y.-M.; Minatoguchi, S.; Mizukami, H.; Fujiwara, H. New sesquiterpene lactones from water extract of the root of *Lindera strychnifolia* with cytotoxicity against the human small cell lung cancer cell, SBC-3. *Tetrahedron Lett.* **2005**, *46*, 8657–8660. [CrossRef]
30. Jang, H.-J.; Oh, H.-M.; Hwang, J.T.; Kim, M.-H.; Lee, S.; Jung, K.; Kim, Y.-H.; Lee, S.W.; Rho, M.-C. Eudesmane-type sesquiterpenoids from *Salvia plebeia* inhibit IL-6-induced STAT3 activation. *Phytochemistry* **2016**, *130*, 335–342. [CrossRef]
31. Liu, Q.; Ahn, J.H.; Kim, S.B.; Lee, C.; Hwang, B.Y.; Lee, M.K. Sesquiterpene lactones from the roots of *Lindera strychnifolia*. *Phytochemistry* **2013**, *87*, 112–118. [CrossRef] [PubMed]
32. Liu, Y.; Ma, J.; Wang, Y.; Donkor, P.O.; Li, Q.; Gao, S.; Hou, Y.; Xu, Y.; Cui, J.; Ding, L. Eudesmane-type sesquiterpenes from *Curcuma phaeocaulis* and their inhibitory activities on nitric oxide production in RAW 264.7 cells. *Eur. J. Org. Chem.* **2014**, *2014*, 5540–5548. [CrossRef]
33. Buděšínský, M.; Holub, M.; Šaman, D.; Smítalová, Z.; Ulubelen, A.; Öksüz, S. Structure of istanbulin A and istanbulin B—Two sesquiterpenic lactones from *Smyrnium olusatrum* L. *Collect. Czech. Chem. Commun.* **1984**, *49*, 1311–1317. [CrossRef]
34. Xu, Y.-J.; Tang, C.-P.; Tan, M.-J.; Ke, C.-Q.; Wu, T.; Ye, Y. Sesquiterpenoids and diterpenoids from *Chloranthus anhuiensis*. *Chem. Biodivers.* **2010**, *7*, 151–157. [CrossRef] [PubMed]
35. Schroeder, G.; Rohmer, M.; Beck, J.P.; Anton, R. 7-Oxo-, 7α-hydroxy- and 7β-hydroxysterols from *Euphorbia fischeriana*. *Phytochemistry* **1980**, *19*, 2213–2215. [CrossRef]
36. Shen, T.; Zhang, L.; Wang, Y.-Y.; Fan, P.-H.; Wang, X.-N.; Lin, Z.-M.; Lou, H.-X. Steroids from *Commiphora mukul* display antiproliferative effect against human prostate cancer PC3 cells via induction of apoptosis. *Bioorg. Med. Chem. Lett.* **2012**, *22*, 4801–4806. [CrossRef]
37. Brieskorn, C.H.; Noble, P. Drei neue Furanogermacrene aus Myrrhe. *Tetrahedron Lett.* **1980**, *21*, 1511–1514. [CrossRef]
38. Santoro, E.; Messina, F.; Marcotullio, M.C.; Superchi, S. Absolute configuration of bioactive furanogermacrenones from *Commiphora erythraea* (Ehrenb) Engl. by computational analysis of their chiroptical properties. *Tetrahedron* **2014**, *70*, 8033–8039. [CrossRef]
39. Greve, H.L.; Kaiser, M.; Schmidt, T.J. Investigation of antiplasmodial effects of terpenoid compounds isolated from myrrh. *Planta Med.* **2020**, *86*, 643–654. [CrossRef]
40. Takeda, K.; Horibe, I.; Minato, H. Components of the root of *Lindera strychnifolia* Vill. Part XIV. Sesquiterpene lactones from the root of *Lindera strychnifolia* Vill. *J. Chem. Soc.* **1968**, 569–572. [CrossRef]
41. Tada, H.; Minato, H.; Takeda, K. Components of the root of *Lindera strychnifolia* Vill. Part XVIII. Neosericenyl acetate and dehydrolindestrenolide. *J. Chem. Soc. C* **1971**, 1070–1073. [CrossRef]
42. Oshima, Y.; Iwakawa, T.; Hikino, H. Alismol and alismoxide, sesquiterpenoids of *Alisma* rhizomes. *Phytochemistry* **1983**, *22*, 183–185. [CrossRef]
43. Hikino, H.; Konno, C.; Agatsuma, K.; Takemoto, T.; Horibe, I.; Tori, K.; Ueyama, M.; Takeda, K. Sesquiterpenoids. Part XLVII. Structure, configuration, conformation, and thermal rearrangement of furanodienone, isofuranodienone, curzerenone, epicurzerenone, and pyrocurzerenone, sesquiterpenoids of *Curcuma zedoaria*. *J. Chem. Soc. Perkin Trans. 1* **1975**, 478–484. [CrossRef]
44. Brieskorn, C.H.; Noble, P. Furanosesquiterpenes from the essential oil of myrrh. *Phytochemistry* **1983**, *22*, 1207–1211. [CrossRef]
45. Zhu, N.; Sheng, S.; Sang, S.; Rosen, R.T.; Ho, C.-T. Isolation and characterization of several aromatic sesquiterpenes from *Commiphora myrrha*. *Flavour Fragr. J.* **2003**, *18*, 282–285. [CrossRef]
46. Zhu, N.; Kikuzaki, H.; Sheng, S.; Sang, S.; Rafi, M.M.; Wang, M.; Nakatani, N.; DiPaola, R.S.; Rosen, R.T.; Ho, C.-T. Furanosesquiterpenoids of *Commiphora myrrha*. *J. Nat. Prod.* **2001**, *64*, 1460–1462. [CrossRef]

47. Stahl, E.; Datta, S.N. Neue sesquiterpenoide Inhaltsstoffe der Gundelrebe (*Glechoma hederacea* L.). *Liebigs Ann. Chem.* **1972**, *757*, 23–32. [CrossRef]
48. Tashkhodzhaev, B.; Abduazimov, B.K. Stereochemistry of sesquiterpenes of the germacrane type. *Chem. Nat. Compd.* **1997**, *33*, 382–388. [CrossRef]
49. Chaturvedula, V.P.; Schilling, J.K.; Miller, J.S.; Andriantsiferana, R.; Rasamison, V.E.; Kingston, D.G.I. New cytotoxic terpenoids from the wood of *Vepris punctata* from the Madagascar Rainforest. *J. Nat. Prod.* **2004**, *67*, 895–898. [CrossRef]
50. Yamakawa, K.; Nishitani, K.; Murakami, A.; Yamamoto, A. Studies on the terpenoids and related alicyclic compounds. XXVIII. Chemical transformations of α-santonin into C-8 lactonized eudesmanolides: Yomogin and diastereoisomers of dihydrograveolide. *Chem. Pharm. Bull.* **1983**, *31*, 3397–3410. [CrossRef]
51. Liu, L.-L.; Yang, J.-L.; Shi, Y.-P. Sesquiterpenoids and other constituents from the flower buds of *Tussilago farfara*. *J. Asian Nat. Prod. Res.* **2011**, *13*, 920–929. [CrossRef] [PubMed]
52. Provan, G.J.; Waterman, P.G. Major triterpenes from the resins of *Commiphora incisa* and *C. kua* and their potential chemotaxonomic significance. *Phytochemistry* **1988**, *27*, 3841–3843. [CrossRef]
53. Shen, T.; Yuan, H.-Q.; Wan, W.-Z.; Wang, X.-L.; Wang, X.-N.; Ji, M.; Lou, H.-X. Cycloartane-type triterpenoids from the resinous exudates of *Commiphora opobalsamum*. *J. Nat. Prod.* **2008**, *71*, 81–86. [CrossRef] [PubMed]
54. Chowdhury, R.; Rashid, R.B.; Sohrab, M.H.; Hasan, C.M. 12α-Hydroxystigmast-4-en-3-one: A new bioactive steroid from *Toona ciliata* (Meliaceae). *Pharmazie* **2003**, *58*, 272–273. [CrossRef] [PubMed]
55. Dhal, R.; Lalami, K.; Brown, E. Racemic total syntheses of isoaustrobailignan-1 and of some related aryltetralin lactones. *Org. Prep. Proced. Int.* **1989**, *21*, 109–118. [CrossRef]
56. Baser, K.H.C.; Demirci, B.; Dekebo, A.; Dagne, E. Essential oils of some *Boswellia* spp., myrrh and opopanax. *Flavour Fragr. J.* **2003**, *18*, 153–156. [CrossRef]
57. Tsui, W.-Y.; Brown, G.D. Cycloeudesmanolides from *Sarcandra glabra*. *Phytochemistry* **1996**, *43*, 819–821. [CrossRef]
58. Guella, G.; Skropeta, D.; Mancini, I.; Pietra, F. The first 6,8-cycloeudesmane sesquiterpene from a marine organism: The red seaweed *Laurencia microcladia* from the Baia di Calenzana, Elba Island. *Z. Naturforsch. B* **2002**, *57*, 1147–1151. [CrossRef]
59. Ahmed, F.; Ali, M.; Singh, O. New compounds from *Commiphora myrrha* (Nees) Engl. *Pharmazie* **2006**, *61*, 728–731. [CrossRef]
60. Woyengo, T.A.; Ramprasath, V.R.; Jones, P.J.H. Anticancer effects of phytosterols. *Eur. J. Clin. Nutr.* **2009**, *63*, 813–820. [CrossRef]
61. Provan, G.J.; Waterman, P.G. Picropolygamain: A new lignan from *Commiphora incisa* resin[1,2]. *Planta Med.* **1985**, *51*, 271–272. [CrossRef]
62. Dekebo, A.; Lang, M.; Polborn, K.; Dagne, E.; Steglich, W. Four lignans from *Commiphora erlangeriana*. *J. Nat. Prod.* **2002**, *65*, 1252–1257. [CrossRef] [PubMed]
63. Habtemariam, S. Cytotoxic and cytostatic activity of erlangerins from *Commiphora erlangeriana*. *Toxicon* **2003**, *41*, 723–727. [CrossRef]
64. Vissiennon, C.; Hammoud, D.; Goos, K.-H.; Nieber, K.; Arnhold, J. Synergistic interactions of chamomile flower, myrrh and coffee charcoal in inhibiting pro-inflammatory chemokine release from activated human macrophages. *Planta Med.* **2017**, *4*, 13–18. [CrossRef]
65. Jang, H.-J.; Lee, S.; Lee, S.-J.; Lim, H.-J.; Jung, K.; Kim, Y.H.; Lee, S.W.; Rho, M.-C. Anti-inflammatory activity of eudesmane-type sesquiterpenoids from *Salvia plebeia*. *J. Nat. Prod.* **2017**, *80*, 2666–2676. [CrossRef]
66. Xu, J.; Jin, D.; Shi, D.; Ma, Y.; Yang, B.; Zhao, P.; Guo, Y. Sesquiterpenes from *Vladimiria souliei* and their inhibitory effects on NO production. *Fitoterapia* **2011**, *82*, 508–511. [CrossRef] [PubMed]
67. Dekebo, A.; Dagne, E.; Sterner, O. Furanosesquiterpenes from *Commiphora sphaerocarpa* and related adulterants of true myrrh. *Fitoterapia* **2002**, *73*, 48–55. [CrossRef]
68. Morteza-Semnani, K.; Saeedi, M. Constituents of the essential oil of *Commiphora myrrha* (Nees) Engl. var. *molmol*. *J. Essent. Oil Res.* **2003**, *15*, 50–51. [CrossRef]
69. Dolara, P.; Moneti, G.; Pieraccini, G.; Romanelli, N. Characterization of the action on central opioid receptors of furaneudesma-1,3-diene, a sesquiterpene extracted from myrrh. *Phytother. Res.* **1996**, *1996*, 81–83.
70. Paço, A.; Brás, T.; Santos, J.O.; Sampaio, P.; Gomes, A.C.; Duarte, M.F. Anti-inflammatory and immunoregulatory action of sesquiterpene lactones. *Molecules* **2022**, *27*, 1142. [CrossRef]
71. Dirsch, V.M.; Stuppner, H.; Ellmerer-Müller, E.P.; Vollmar, A.M. Structural requirements of sesquiterpene lactones to inhibit LPS-induced nitric oxide synthesis in RAW 264.7 macrophages. *Bioorg. Med. Chem.* **2000**, *8*, 2747–2753. [CrossRef] [PubMed]
72. Marston, A.; Borel, C.; Hostettmann, K. Separation of natural products by centrifugal partition chromatography. *J. Chromatogr. A* **1988**, *450*, 91–99. [CrossRef]
73. Chen, M.; Lou, Y.; Wu, Y.; Meng, Z.; Li, L.; Yu, L.; Zeng, S.; Zhou, H.; Jiang, H. Characterization of in vivo and in vitro metabolites of furanodiene in rats by high performance liquid chromatography–electrospray ionization mass spectrometry and nuclear magnetic resonance spectra. *J. Pharm. Biomed. Anal.* **2013**, *86*, 161–168. [CrossRef] [PubMed]
74. Glauco, M.B.; Jorge, B.R.; Arlett, M.P.; Samuel, P.T.; Luis, A.M. An eremophilanolide from *Senecio rosmarinus*. *Phytochemistry* **1986**, *25*, 2412–2414. [CrossRef]
75. Thinh, N.S.; Thu, N.T.B.; Trang, D.T.; van Kiem, P.; Tai, B.H.; Nhiem, N.X. Sesquiterpenes from *Fissistigma pallens* (Fin. & Gagn.) Merr. *Vietnam J. Chem.* **2019**, *57*, 552–557. [CrossRef]

76. Li, R.-J.; Guo, D.-X.; Lou, H.-X. A new guaiane-type sesquiterpene lactone from the Chinese liverwort *Porella acutifolia* subsp. *tosana*. *Chin. J. Nat. Med.* **2014**, *11*, 74–76. [CrossRef]
77. Mosmann, T. Rapid colorimetric assay for cellular growth and survival: Application to proliferation and cytotoxicity assays. *J. Immunol. Methods* **1983**, *65*, 55–63. [CrossRef]